
Wasserstein K -means for clustering probability distributions

Yubo Zhuang, Xiaohui Chen, Yun Yang
Department of Statistics
University of Illinois at Urbana-Champaign
{yubo2,xhchen,yy84}@illinois.edu

Abstract

Clustering is an important exploratory data analysis technique to group objects based on their similarity. The widely used K -means clustering method relies on some notion of distance to partition data into a fewer number of groups. In the Euclidean space, centroid-based and distance-based formulations of the K -means are equivalent. In modern machine learning applications, data often arise as probability distributions and a natural generalization to handle measure-valued data is to use the optimal transport metric. Due to non-negative Alexandrov curvature of the Wasserstein space, barycenters suffer from regularity and non-robustness issues. The peculiar behaviors of Wasserstein barycenters may make the centroid-based formulation fail to represent the within-cluster data points, while the more direct distance-based K -means approach and its semidefinite program (SDP) relaxation are capable of recovering the true cluster labels. In the special case of clustering Gaussian distributions, we show that the SDP relaxed Wasserstein K -means can achieve exact recovery given the clusters are well-separated under the 2-Wasserstein metric. Our simulation and real data examples also demonstrate that distance-based K -means can achieve better classification performance over the standard centroid-based K -means for clustering probability distributions and images.

1 Introduction

Clustering is a major tool for unsupervised machine learning problems and exploratory data analysis in statistics. Suppose we observe a sample of data points X_1, \dots, X_n taking values in a metric space $(\mathcal{X}, \|\cdot\|)$. Suppose there exists a clustering structure G_1^*, \dots, G_K^* such that each data point X_i belongs to exactly one of the unknown cluster G_k^* . The goal of clustering analysis is to recover the true clusters G_1^*, \dots, G_K^* given the input data X_1, \dots, X_n . In the Euclidean space $\mathcal{X} = \mathbb{R}^p$, the K -means clustering is a widely used method that achieves the empirical success in many applications [MacQueen, 1967]. In modern machine learning and data science problems such as computer graphics [Solomon et al., 2015], data exhibits complex geometric features and traditional clustering methods developed for Euclidean data may not be well suited to analyze such data.

In this paper, we consider the clustering problem of probability measures μ_1, \dots, μ_n into K groups. As a motivating example, the MNIST dataset contains images of handwritten digits 0-9. Normalizing the greyscale images into histograms as probability measures, a common task is to cluster the images. One can certainly apply the Euclidean K -means to the vectorized images. However, this would lose important geometric information of the two-dimensional data. On the other hand, theory of optimal transport [Villani, 2003] provides an appealing framework to model measure-valued data as probabilities in many statistical tasks [Domazakis et al., 2019, Chen et al., 2021, Bigot et al., 2017, Seguy and Cuturi, 2015, Rigollet and Weed, 2019, Hütter and Rigollet, 2019, Cazelles et al., 2018].

Background on K -means clustering. Algorithmically, the K -means clustering have two equivalent formulations in the Euclidean space – centroid-based and distance-based – in the sense that they both yield the same partition estimate for the true clustering structure. Given the Euclidean data $X_1, \dots, X_n \in \mathbb{R}^p$, the *centroid-based* formulation of standard K -means can be expressed as

$$\min_{\beta_1, \dots, \beta_K \in \mathbb{R}^d} \sum_{i=1}^n \min_{k \in [K]} \|X_i - \beta_k\|_2^2 = \min_{G_1, \dots, G_K} \left\{ \sum_{k=1}^K \sum_{i \in G_k} \|X_i - \bar{X}_k\|_2^2 : \bigsqcup_{k=1}^K G_k = [n] \right\}, \quad (1)$$

where clusters $\{G_k\}_{k=1}^K$ are determined by the Voronoi diagram from $\{\beta_k\}_{k=1}^K$, $\bar{X}_k = |G_k|^{-1} \sum_{i \in G_k} X_i$ denotes the centroid of cluster G_k , \bigsqcup denotes the disjoint union and $[n] = \{1, \dots, n\}$. Heuristic algorithm for solving (1) includes Lloyd’s algorithm [Lloyd, 1982], which is an iterative procedure alternating the partition and centroid estimation steps. Specifically, given an initial centroid estimate $\beta_1^{(1)}, \dots, \beta_K^{(1)}$, one first assigns each data point to its nearest centroid at the t -th iteration according to the Voronoi diagram, i.e.,

$$G_k^{(t)} = \left\{ i \in [n] : \|X_i - \beta_k^{(t)}\|_2 \leq \|X_i - \beta_j^{(t)}\|_2, \forall j \in [K] \right\}, \quad (2)$$

and then update the centroid for each cluster

$$\beta_k^{(t+1)} = \frac{1}{|G_k^{(t)}|} \sum_{i \in G_k^{(t)}} X_i, \quad (3)$$

where $|G_k^{(t)}|$ denotes the cardinality of $G_k^{(t)}$. Step (2) and step (3) alternate until convergence.

The *distance-based* (sometimes also referred as *partition-based*) formulation directly solves the following constrained optimization problem without referring to the estimated centroids:

$$\min_{G_1, \dots, G_K} \left\{ \sum_{k=1}^K \frac{1}{|G_k|} \sum_{i, j \in G_k} \|X_i - X_j\|_2^2 : \bigsqcup_{k=1}^K G_k = [n] \right\}. \quad (4)$$

Observe that (1) with nearest centroid assignment and (4) are equivalent for the clustering purpose due to the following identity, which extends the parallelogram law from two points to n points,

$$\sum_{i, j=1}^n \|X_i - X_j\|_2^2 = 2n \sum_{i=1}^n \|X_i - \bar{X}\|_2^2, \quad \text{with } \bar{X} = \frac{1}{n} \sum_{i=1}^n X_i \quad \text{and } X_i \in \mathbb{R}^p. \quad (5)$$

Consequently, the two criteria yield the same partition estimate for G_1^*, \dots, G_K^* . The key identity (5) establishing the equivalence relies on two facts of the Euclidean space: (i) it is a vector space (i.e., vectors can be averaged in the linear sense); (ii) it is flat (i.e., zero curvature), both of which are unfortunately not true for the Wasserstein space $(\mathcal{P}_2(\mathbb{R}^p), W_2)$ that endows the space $\mathcal{P}_2(\mathbb{R}^p)$ of all probability distributions with finite second moments with the 2-Wasserstein metric W_2 [Ambrosio et al., 2005]. In particular, the 2-Wasserstein distance between two distributions μ and ν in $\mathcal{P}_2(\mathbb{R}^p)$ is defined as

$$W_2^2(\mu, \nu) := \min_{\gamma} \left\{ \int_{\mathbb{R}^p \times \mathbb{R}^p} \|x - y\|_2^2 d\gamma(x, y) \right\}, \quad (6)$$

where minimization over γ runs over all possible couplings with marginals μ and ν . It is well-known that the Wasserstein space is a metric space (in fact a geodesic space) with non-negative curvature in the Alexandrov sense [Lott, 2008].

Our contributions. We summarize our main contributions as followings: (i) we provide evidence for pitfalls (irregularity and non-robustness) of barycenter-based Wasserstein K -means, both theoretically and empirically, and (ii) we generalize the distance-based formulation of K -means to the Wasserstein space and establish the exact recovery property of its SDP relaxation for clustering Gaussian measures under a separateness lower bound in the 2-Wasserstein distance.

Existing work. Since the K -means clustering is a worst-case NP-hard problem [Aloise et al., 2009], approximation algorithms have been extensively studied in literature including: Lloyd’s algorithm [Lloyd, 1982], spectral methods [von Luxburg, 2007, Meila and Shi, 2001, Ng et al., 2001], semidefinite programming (SDP) relaxations [Peng and Wei, 2007], non-convex methods via

low-rank matrix factorization [Burer and Monteiro, 2003]. Theoretic guarantees of those methods are established for statistical models on Euclidean data [Lu and Zhou, 2016, von Luxburg et al., 2008, Vempala and Wang, 2004, Fei and Chen, 2018, Giraud and Verzelen, 2018, Chen and Yang, 2021, Zhuang et al., 2022].

The concept of clustering general measure-valued data is introduced by Domazakis et al. [2019], where the authors proposed the centroid-based Wasserstein K-means algorithm. It replaced the Euclidean norm and sample means by the Wasserstein distance and barycenters respectively. Verdinelli and Wasserman [2019] proposed a modified Wasserstein distance for distribution clustering. And after that, Chazal et al. [2021] proposed a method in Clustering of measures via mean measure quantization by first vectorizing the measures in a finite Euclidean space followed by an efficient clustering algorithm such as single-linkage clustering with L_∞ distance. The vectorization methods could improve the computational efficiency but might not capture the properties of probability measures well compared to clustering algorithms based directly on Wasserstein space.

2 Wasserstein K -means clustering methods

In this section, we generalize the Euclidean K -means to the Wasserstein space. Our starting point is to mimic the standard K -means methods for Euclidean data. Thus we may define two versions of the Wasserstein K -means clustering formulations: *centroid-based* and *distance-based*. As we mentioned in Section 1, when working with Wasserstein space $(\mathcal{P}_2(\mathbb{R}^p), W_2)$, the corresponding centroid-based criterion (1) and the distance-based criterion (4), where the Euclidean metric $\|\cdot\|_2$ is replaced with the 2-Wasserstein metric W_2 , may lead to radically different clustering schemes. To begin with, we would like to argue that due to the irregularity and non-robustness of barycenters in the Wasserstein space, the centroid-based criterion may lead to unreasonable clustering schemes that lack physical interpretations and are sensitive to small data perturbations.

2.1 Clustering based on barycenters

The centroid-based Wasserstein K -means for extending the Lloyd’s algorithm into the Wasserstein space has been recently considered by Domazakis et al. [2019]. Specifically, it is an iterative algorithm proceeds as following. Given an initial centroid estimate $\nu_1^{(1)}, \dots, \nu_K^{(1)}$, one first assigns each probability measure μ_1, \dots, μ_n to its nearest centroid in the Wasserstein geometry at the t -th iteration according to the Voronoi diagram:

$$G_k^{(t)} = \left\{ i \in [n] : W_2(\mu_i, \nu_k^{(t)}) \leq W_2(\mu_i, \nu_j^{(t)}), \quad \forall j \in [K] \right\}, \quad (7)$$

and then update the centroid for each cluster

$$\nu_k^{(t+1)} = \arg \min_{\nu \in \mathcal{P}_2(\mathbb{R}^d)} \frac{1}{|G_k^{(t)}|} \sum_{i \in G_k^{(t)}} W_2^2(\mu_i, \nu). \quad (8)$$

Note that $\nu_k^{(t+1)}$ in (8) is referred as *barycenter* of probability measures $\mu_i, i \in G_k^{(t)}$, a Wasserstein analog of the Euclidean average or mean [Agueh and Carlier, 2011]. We will also ex-changeably use barycenter-based K -means to mean the centroid-based K -means in the Wasserstein space. Even though the Wasserstein barycenter is a natural notion of averaging probability measures, it may exhibit peculiar behaviours and fail to represent the within-cluster data points, partly due to the violation of the generalized parallelogram law (5) (for non-flat spaces) if the Euclidean metric $\|\cdot\|_2$ is replaced with the 2-Wasserstein metric W_2 .

Example 1 (Irregularity of Wasserstein barycenters). Wasserstein barycenter has much less regularity than the sample mean in the Euclidean space [Kim and Pass, 2017]. In particular, Santambrogio and Wang [2016] constructed a simple example of two probability measures that are supported on line segments in \mathbb{R}^2 , whereas the support of their barycenter obtained as the displacement interpolation the two endpoint probability measures is not convex (cf. left plot in Figure 1). In this example, the probability density μ_0 and μ_1 are supported on the line segments $L_0 = \{(s, as) : s \in [-1, 1]\}$ and $L_1 = \{(s, -as) : s \in [-1, 1]\}$ respectively. We choose $a \in (0, 1)$ to identify the orientation of L_0 and L_1 based on the x -axis. Moreover, we consider the linear density functions $\mu_0(s) = (1 - s)/2$

and $\mu_1(s) = (1 + s)/2$ for $s \in [-1, 1]$ supported on L_0 and L_1 respectively. Then the optimal transport map $T := T_{\mu_0 \rightarrow \mu_1}$ from μ_0 to μ_1 is given by

$$T(x, ax) = \left(-1 + \sqrt{4 - (1 - x)^2}, -a \cdot (-1 + \sqrt{4 - (1 - x)^2}) \right), \quad (9)$$

and the barycenter corresponds to the displacement interpolation $\mu_t = [(1 - t)\text{id} + tT]_{\#}\mu_0$ at $t = 0.5$ [McCann, 1997]. For self-contained purpose, we give the proof of (9) in Appendix D.1. Fig. 1 on the left shows the support of barycenter $\mu_{0.5}$ is not convex (in fact part of an ellipse boundary) even though the supports of μ_0 and μ_1 are convex. This example shows that the barycenter functional is not geodesically convex in the Wasserstein space. As barycenters turn out to be essential in centroid-based Wasserstein K -means and irregularity of the barycenter may fail to represent the cluster (see more details in Example 3 and Remark 9 below), this counter-example is our motivation to seek alternative formulation. ■

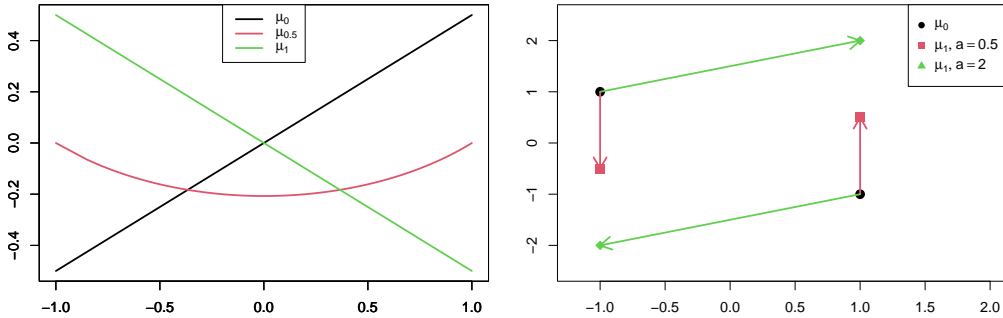


Figure 1: Left: support of the Wasserstein barycenter as the displacement interpolation between μ_0 and μ_1 at $t = 0.5$ in Example 1. Right: non-robustness of the optimal transport map (arrow lines) and Wasserstein barycenter w.r.t. small perturbation around $a = 1$ for the target measure in Example 2.

Example 2 (Non-robustness of Wasserstein barycenters). Another unappealing feature of the Wasserstein barycenter is its sensitivity to data perturbation: a small (local) change in one contributing probability measure may lead to large (global) changes in the resulting barycenter. See Fig. 1 on the right for such an example. In this example, we take the source measure as $\mu_0 = 0.5 \delta_{(-1,1)} + 0.5 \delta_{(1,-1)}$ and the target measure as $\mu_1 = 0.5 \delta_{(-1,-a)} + 0.5 \delta_{(1,a)}$ for some $a > 0$. It is easy to see that the optimal transport map $T := T_{\mu_0 \rightarrow \mu_1}$ has a dichotomy behavior:

$$T(-1, 1) = \begin{cases} (-1, -a) & \text{if } 0 < a < 1 \\ (1, a) & \text{if } a > 1 \end{cases} \quad \text{and} \quad T(1, -1) = \begin{cases} (1, a) & \text{if } 0 < a < 1 \\ (-1, -a) & \text{if } a > 1 \end{cases}. \quad (10)$$

Thus the Wasserstein barycenter determined by the displacement interpolation $\mu_t = [(1 - t)\text{id} + tT]_{\#}\mu_0$ is a discontinuous function at $a = 1$. This non-robustness can be attribute to the discontinuity of the Wasserstein barycenter as a function of its input probability measures; in contrast, the Euclidean mean is a globally Lipschitz continuous function of its input points. ■

Because of these pitfalls of the Wasserstein barycenter shown in Examples 1 and 2, the centroid-based Wasserstein K -means approach described at the beginning of this subsection may lead to unreasonable and unstable clustering schemes. In addition, an ill-conditioned configuration may significantly slow down the convergence of commonly used barycenter approximating algorithms such as iterative Bregman projections [Benamou et al., 2015]. Below, we give a concrete example of such phenomenon in the clustering context.

Example 3 (Failure of centroid-based Wasserstein K -means). In a nutshell, the failure in this example is due to the counter-intuitive phenomenon illustrated in the right panel of Fig. 2, where some distribution μ_3 in the Wasserstein space may have larger W_2 distance to Wasserstein barycenter μ_1^* than every distribution μ_i ($i = 1, 2$) that together forms it. As a result of this strange configuration, even though μ_3 is closer to μ_1 and μ_2 from the first cluster with barycenter μ_1^* than μ_4 coming from a second cluster with barycenter μ_2^* , it will be incorrectly assigned to the second cluster using the centroid-based criterion (7), since $W_2(\mu_3, \mu_1^*) > W_2(\mu_3, \mu_2^*) > \max \{W_2(\mu_3, \mu_1), W_2(\mu_3, \mu_2)\}$. In contrast, for Euclidean spaces due to the following equivalent formulation of the generalized

parallelogram law (5),

$$\sum_{i=1}^n \|X - X_i\|_2^2 = n\|X - \bar{X}\|_2^2 + \sum_{i=1}^n \|X_i - \bar{X}\|_2^2 \geq n\|X - \bar{X}\|_2^2, \quad \text{for any } X \in \mathbb{R}^p,$$

there is always some point X_{i^\dagger} satisfying $\|X - X_{i^\dagger}\|_2 \geq \|X - \bar{X}\|_2$, that is, further away from X than the mean \bar{X} ; thereby excluding counter-intuitive phenomena as the one shown in Fig. 2.

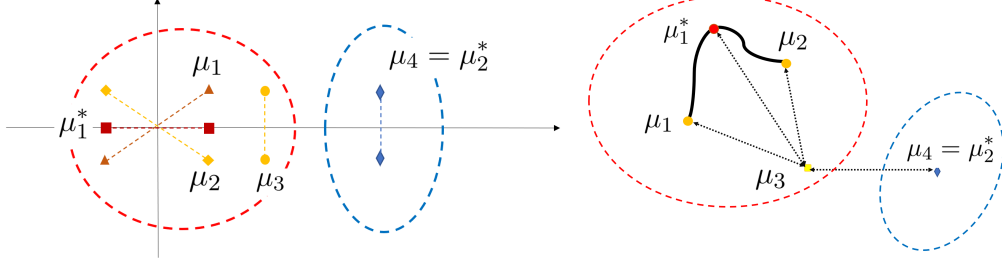


Figure 2: Left: visualization of Example 3 in \mathbb{R}^2 and Wasserstein space. Right: the black curve connecting μ_1 and μ_2 depicts the geodesic between them.

Concretely, the first cluster G_1^* is shown in the left panel of Fig. 2 highlighted by a red circle, consisting of m copies of (μ_1, μ_2) pairs and one copy of μ_3 ; the second cluster G_2^* containing copies of μ_4 is highlighted by a blue circle. Each distribution assigns equal probability mass to two points, where the two supporting points are connected by a dashed line for easy illustration. More specifically, we set

$$\begin{aligned} \mu_1 &= 0.5 \delta_{(x,y)} + 0.5 \delta_{(-x,-y)}, & \mu_2 &= 0.5 \delta_{(x,-y)} + 0.5 \delta_{(-x,y)}, \\ \mu_3 &= 0.5 \delta_{(x+\epsilon_1,y)} + 0.5 \delta_{(x+\epsilon_1,-y)}, & \text{and } \mu_4 &= 0.5 \delta_{(x+\epsilon_1+\epsilon_2,y)} + 0.5 \delta_{(x+\epsilon_1+\epsilon_2,-y)}, \end{aligned}$$

where $\delta_{(x,y)}$ denotes the point mass measure at point (x, y) , and $(x, y, \epsilon_1, \epsilon_2)$ are positive constants. The property of this configuration can be summarized by the following lemma.

Lemma 4 (Configuration characterization). If $(x, y, \epsilon_1, \epsilon_2)$ satisfies

$$y^2 < \min\{x^2, 0.25 \Delta_{\epsilon_1, x}\} \quad \text{and} \quad \Delta_{\epsilon_1, x} < \epsilon_2^2 < \Delta_{\epsilon_1, x} + y^2,$$

where $\Delta_{\epsilon_1, x} := \epsilon_1^2 + 2x^2 + 2x\epsilon_1$, then for all sufficiently large m (number of copies of μ_1 and μ_2),

$$W_2(\mu_3, \mu_2^*) < W_2(\mu_3, \mu_1^*) \quad \text{and} \quad \underbrace{\max_{k=1,2} \max_{i,j \in G_k} W_2(\mu_i, \mu_j)}_{\text{largest within-cluster distance}} < \underbrace{\min_{i \in G_1, j \in G_2} W_2(\mu_i, \mu_j)}_{\text{least between-cluster distance}},$$

where μ_k^* denotes the Wasserstein barycenter of cluster G_k for $k = 1, 2$.

Note that the condition of Lemma 4 implies $y < x$. Therefore, the barycenter between μ_1 and μ_2 is $\tilde{\mu}_1^* := 0.5 \delta_{(x,0)} + 0.5 \delta_{(-x,0)}$ lying on the horizontal axis. By increasing m , the barycenter μ_1^* of cluster G_1^* can be made arbitrarily close to $\tilde{\mu}_1^*$. The second inequality in Lemma 4 shows that all within-cluster distances are strictly less than the between-cluster distances; therefore, clustering based on pairwise distances is able to correctly recover the cluster label of μ_3 . However, since μ_3 is closer to the barycenter μ_2^* of cluster G_2^* according to the first inequality in Lemma 4, it will be mis-classified into G_2^* using the centroid-based criterion. We emphasize that cluster positions in this example are generic and do exist in real data; see Remark 9 and Section 4.3 for further discussions on our experiment results on MNIST data. Moreover, similar to Example 2, a small change in the orientation of distribution μ_1 may completely alter the clustering membership of μ_3 based on the centroid criterion. Specifically, if we slightly increase x to make it exceed y , then the barycenter between μ_1 and μ_2 becomes $\tilde{\mu}_1^* := 0.5 \delta_{(0,y)} + 0.5 \delta_{(0,-y)}$ that lies on the vertical axis. Correspondingly, if based on centroids, then μ_3 should be clustered into G_1^* as it is closer to the barycenter μ_1^* of G_1^* than the barycenter μ_2^* of G_2^* . Therefore, the centroid-based criterion can be unstable against data perturbations. In comparison, a pairwise distances based criterion always assigns μ_3 into cluster G_2^* no matter $x < y$ or $x > y$. ■

2.2 Clustering based on pairwise distances

Due to the irregularity and non-robustness of centroid-based Wasserstein K -means, we instead propose and advocate the use of distance-based Wasserstein K -means below, which extends the Euclidean distance-based K -means formulation (4) into the Wasserstein space,

$$\min_{G_1, \dots, G_K} \left\{ \sum_{k=1}^K \frac{1}{|G_k|} \sum_{i, j \in G_k} W_2^2(\mu_i, \mu_j) : \bigsqcup_{k=1}^K G_k = [n] \right\}. \quad (11)$$

Correspondingly, we can analogously design a greedy algorithm resembling the Wasserstein Lloyd's algorithm described in Section 2.1 that solves the centroid-based Wasserstein K -means. Specifically, the greedy algorithm proceeds in an iterative manner as following. Given an initial cluster membership estimate $G_1^{(1)}, \dots, G_K^{(1)}$, one assigns each probability measure μ_1, \dots, μ_n based on minimizing the averaged squared W_2 distances to all current members in every cluster, leading to an updated cluster membership estimate

$$G_k^{(t+1)} = \left\{ i \in [n] : \frac{1}{|G_k^{(t)}|} \sum_{s \in G_k^{(t)}} W_2^2(\mu_i, \mu_s) \leq \frac{1}{|G_j^{(t)}|} \sum_{s \in G_j^{(t)}} W_2^2(\mu_i, \mu_s), \quad \forall j \in [K] \right\}. \quad (12)$$

We arbitrarily select among the least W_2 distance clusters in the case of a tie. We highlight that the center-based and distance-based Wasserstein K -means formulations may not necessarily be equivalent to yield the same cluster labels (cf. Example 3). Below, we shall give some example illustrating connections to the standard K -means clustering in the Euclidean space.

Example 5 (Degenerate probability measures). If the probability measures are Dirac at point $X_i \in \mathbb{R}^p$, i.e., $\mu_i = \delta_{X_i}$, then the Wasserstein K -means is the same as the standard K -means since $W_2(\mu_i, \mu_j) = \|X_i - X_j\|_2$. ■

Example 6 (Gaussian measures). If $\mu_i = N(m_i, V_i)$ with positive-definite covariance matrices $\Sigma_i \succ 0$, then the squared 2-Wasserstein distance can be expressed as the sum of the squared Euclidean distance on the mean vector and

$$d^2(V_i, V_j) = \text{Tr} \left[V_i + V_j - 2 \left(V_i^{1/2} V_j V_i^{1/2} \right)^{1/2} \right], \quad (13)$$

the squared *Bures distance* on the covariance matrix [Bhatia et al., 2019]. Here, we use $V^{1/2}$ to denote the unique symmetric square root matrix of $V \succ 0$. That is,

$$W_2^2(\mu_i, \mu_j) = \|m_i - m_j\|_2^2 + d^2(V_i, V_j). \quad (14)$$

Then the Wasserstein K -means, formulated either in (7) or (11), can be viewed as a *covariance-adjusted* Euclidean K -means by taking account into the shape or orientation information in the (non-degenerate) Gaussian inputs. ■

Example 7 (One-dimensional probability measures). If μ_i are probability measures on \mathbb{R} with cumulative distribution function (cdf) F_i , then the Wasserstein distance can be written in terms of the *quantile transform*

$$W_2^2(\mu_i, \mu_j) = \int_0^1 [F_i^-(u) - F_j^-(u)]^2 du, \quad (15)$$

where F^- is the generalized inverse of the cdf F on $[0, 1]$ defined as $F^-(u) = \inf\{x \in \mathbb{R} : F(x) > u\}$ (cf. Theorem 2.18 [Villani, 2003]). Thus the one-dimensional probability measures in Wasserstein space can be isometrically embedded in a flat L^2 space, and we can bring back the equivalence of the Wasserstein and Euclidean K -means clustering methods. ■

3 SDP relaxation and its theoretic guarantee

Note that Wasserstein Lloyd's algorithm requires to use and compute the barycenter in (7) and (8) at each iteration, which can be computationally expensive when the domain dimension d is large or the configuration is ill-conditioned (cf. Example 2). On the other hand, it is known that solving the distance-based K -means (4) is worst-case NP-hard for Euclidean data. Thus we expect solving

the distance-based Wasserstein K -means (11) is also computationally hard. A common way is to consider convex relaxations to approximate the solution of (11). It is known that certain SDP relaxation is information-theoretically tight for (4) when the data $X_1, \dots, X_n \in \mathbb{R}^p$ are generated from a Gaussian mixture model with isotropic known variance [Chen and Yang, 2021]. In this paper, we extend the idea into Wasserstein setting for solving (11).

A typical SDP relaxation for Euclidean data uses pairwise inner products to construct an affinity matrix for clustering [Peng and Wei, 2007]; unfortunately, due to the non-flatness nature, a globally well-defined inner product does not exist for Wasserstein spaces with dimension higher than one. Therefore, we will derive a Wasserstein SDP relaxation to the combinatorial optimization problem (4) using the squared distance matrix $A_{n \times n} = \{a_{ij}\}$ with $a_{ij} = W_2^2(\mu_i, \mu_j)$. Concretely, we can one-to-one reparameterize any partition (G_1, \dots, G_K) as a binary *assignment matrix* $H = \{h_{ik}\} \in \{0, 1\}^{n \times K}$ such that $h_{ik} = 1$ if $i \in G_k$ and $h_{ik} = 0$ otherwise. Then (11) can be expressed as a nonlinear 0-1 integer program,

$$\min \left\{ \langle A, HBH^\top \rangle : H \in \{0, 1\}^{n \times K}, H\mathbf{1}_K = \mathbf{1}_n \right\}, \quad (16)$$

where $\mathbf{1}_n$ is the $n \times 1$ vector of all ones and $B = \text{diag}(|G_1|^{-1}, \dots, |G_K|^{-1})$. Changing of variable to the *membership matrix* $Z = HBH^\top$, we note that $Z_{n \times n}$ is a symmetric positive semidefinite (psd) matrix $Z \succeq 0$ such that $\text{Tr}(Z) = K$, $Z\mathbf{1}_n = \mathbf{1}_n$, and $Z \geq 0$ entrywise. Thus we obtain the SDP relaxation of (11) by only preserving these convex constraints:

$$\min_{Z \in \mathbb{R}^{n \times n}} \left\{ \langle A, Z \rangle : Z^\top = Z, Z \succeq 0, \text{Tr}(Z) = K, Z\mathbf{1}_n = \mathbf{1}_n, Z \geq 0 \right\}. \quad (17)$$

To theoretically justify the SDP formulation (17) of Wasserstein K -means, we consider the scenario of clustering Gaussian distributions in Example 6, where the Wasserstein distance (14) contains two separate components: the Euclidean distance on mean vector and the Bures distance (13) on covariance matrix. Without loss of generality, we focus on mean-zero Gaussian distributions since optimal separation conditions for exact recovery based on the Euclidean mean component have been established in [Chen and Yang, 2021]. Suppose we observe Gaussian distributions $\nu_i \sim N(0, V_i)$, $i \in [n]$ from K groups G_1^*, \dots, G_K^* , where cluster G_k^* contains n_k members, and the covariance matrices have the following clustering structure: if $i \in G_k^*$, then

$$V_i = (I + tX_i)V^{(k)}(I + tX_i) \quad \text{with } X_1, \dots, X_n \stackrel{i.i.d.}{\sim} \text{Sym}N(0, 1), \quad (18)$$

where the psd matrix $V^{(k)}$ is the center of the k -th cluster, $\text{Sym}N(0, 1)$ denotes the symmetric random matrix with i.i.d. standard normal entries, and t is a small perturbation parameter such that $(I + tX_i)$ is psd with high probability. For zero-mean Gaussian distributions, we have $W_2(N(0, V), N(0, U)) = d(V, U)$ according to (14). Note that on the Riemannian manifold of psd matrices, the geodesic emanating from $V^{(k)}$ in the direction X as a symmetric matrix can be linearized by $V = (I + tX)V^{(k)}(I + tX)$ in a small neighborhood of t , thus motivating the parameterization of our statistical model in (18). The next theorem gives a separation lower bound to ensure exact recovery of the clustering labels for Gaussian distributions.

Theorem 8 (Exact recovery for clustering Gaussians). Let $\Delta^2 := \min_{k \neq l} d^2(V^{(k)}, V^{(l)})$ denote the minimal pairwise separation among clusters, $\bar{n} := \max_{k \in [K]} n_k$ (and $\underline{n} := \min_{k \in [K]} n_k$) the maximum (minimum) cluster size, and $m := \min_{k \neq l} \frac{2n_k n_l}{n_k + n_l}$ the minimal pairwise harmonic mean of cluster sizes. Suppose the covariance matrix V_i of Gaussian distribution $\nu_i = N(0, V_i)$ is independently drawn from model (18) for $i = 1, 2, \dots, n$. Let $\beta \in (0, 1)$. If the separation Δ^2 satisfies

$$\Delta^2 > \bar{\Delta}^2 := \frac{C_1 t^2}{\min\{(1 - \beta)^2, \beta^2\}} \mathcal{V} p^2 \log n, \quad (19)$$

then the SDP (17) achieves exact recovery with probability at least $1 - C_2 n^{-1}$, provided that

$$\underline{n} \geq C_3 \log^2 n, \quad t \leq C_4 \sqrt{\log n} / [(p + \log \bar{n}) \mathcal{V}^{1/2} T_v^{1/2}], \quad n/m \leq C_5 \log n,$$

where $\mathcal{V} = \max_k \|V^{(k)}\|_{\text{op}}$, $T_v = \max_k \text{Tr}[(V^{(k)})^{-1}]$, and $C_i, i = 1, 2, 3, 4, 5$ are constants.

Remark 9 (Further insight on pitfalls of barycenter-based Wasserstein K -means). Theorem 8 suggests that different from Euclidean data, distributions after centering can be clustered if scales and rotation angles vary (i.e., covariance-adjusted). We further illustrate the rotation and scale effects on

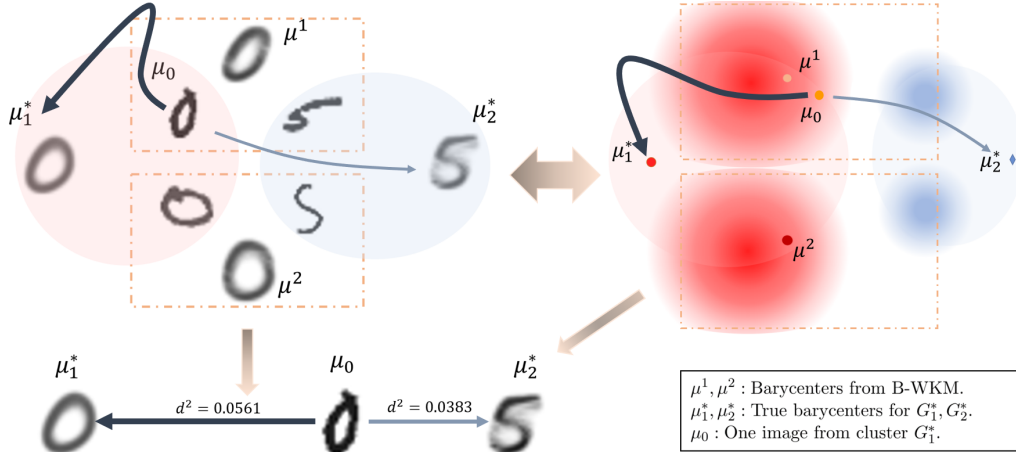


Figure 3: Visualization of misclassification for the barycenter-based Wasserstein K -means (B-WKM) on a randomly sampled subset from MNIST (200 digit "0" and 100 digit "5"). The plot at the bottom is an example of misclassified image. The right plot is the abstraction of the images in the Wasserstein space. The color depth indicates the frequency of the distributions. Red and blue colors stand for distributions belong to true clusters "0" and "5".

the MNIST data that may mislead the centroid-based Wasserstein K -means, thus providing a real data support for Example 3. Here we randomly sample two unbalanced clusters with 200 numbers of "0" and 100 numbers of "5". Fig. 3 shows the clustering results for the centroid-based Wasserstein K -means and its *oracle* version where we replace the estimated barycenters μ_1, μ_2 with the true barycenters μ_1^*, μ_2^* computed on the true labels. Comparing the Wasserstein distances $W_2(\mu_0, \mu_1^*)$ and $W_2(\mu_0, \mu_2^*)$, we see that the image μ_0 (containing digit "0") is closer to μ_2^* (true barycenter of digit "5") and thus it cannot be classified correctly based on the nearest true barycenter (cf. Fig. 3 on the left). Moreover, Wasserstein K -means based on estimated barycenters μ_1, μ_2 yields two clusters of mixed "0" and "5". In both cases, the misclassification error is characterized by grouping similar degrees of angle and/or stretch. Since there are two highly unbalanced clusters of distributions, Wasserstein K -means is likely to enforce larger cluster to separate into two clusters and absorb those around centers (cf. Fig. 3 on the right), leading to larger classification errors. We shall see that in Section 4.3 the distance-based Wasserstein K -means and its SDP relaxation have much smaller classification error rate on MNIST for the reason that we explained in Example 3 (cf. Lemma 4). ■

4 Experiments

4.1 Counter-example in Example 3 revisited

Our first experiment is to back up the claim about the failure of centroid-based Wasserstein K -means in Example 3 through simulations. Instead of using point mass measures that may result in instability for computing the barycenters, we use Gaussian distributions with small variance as a smoothed version. We consider $K = 2$, where cluster G_1^* consists of m_1 many copies of (μ_1, μ_2) pairs and m_2 many μ_3 , and cluster G_2^* consists of m_3 many copies of μ_4 . We choose μ_i as the following two-dimensional mixture of Gaussian distributions $\mu_i = 0.5 N(a_{i,1}, \Sigma_{i,1}) + 0.5 N(a_{i,2}, \Sigma_{i,2})$ for $i = 1, 2, 3, 4$. Due to the space limit, detailed simulation setups and parameters are given in Appendix B. From Table 1, we can observe that Wasserstein SDP has achieved exact recovery for all cases while barycenter-based Wasserstein K -means has only around 40% exact recovery rate among all repetitions. In addition, Wasserstein SDP is more stable than distance-based Wasserstein K -means. Denote $\Delta_k := W^2(\mu_3, \mu_k^*)$ as the squared distance between μ_3 and μ_k^* for $k = 1, 2$, where μ_k^* is the barycenter of G_k^* . Let $\Delta_* := \max_{k=1,2} \max_{i,j \in G_k} W_2(\mu_i, \mu_j)$ and $\Delta^* := \min_{i \in G_1, j \in G_2} W^2(\mu_i, \mu_j)$ be the maximum within-cluster distance and the minimum between-cluster distance respectively. From Table 7 in the Appendix, we can observe that $\Delta_* < \Delta^*$, from which we can expect Wasserstein SDP to correctly cluster all data points in the Wasserstein space. Moreover, Table 1 shows that about 25% times that the distributions (as μ_3) in G_1^* satisfy $\Delta_1 > \Delta_2$, implying those μ_3 to be likely assigned to the wrong cluster, which is consistent with

Example 3. The experiment results also show that any copy of μ_3 is misclassified whenever exact recovery fails for B-WKM, which means the misclassified rate for μ_3 equals to $(1 - \gamma)$, where γ is the exact recovery rate for B-WKM shown in Table 1. Table 6 in the appendix further reports the run time comparison, from which we see that distance-based approaches are more computationally efficient than the barycenter-based one in our settings.

Table 1: Exact recovery rates and frequency of $\Delta_1 > \Delta_2$ for B-WKM among total 50 repetitions in the counter example. W-SDP: Wasserstein SDP, D-WKM: Distance-based Wasserstein K -means, B-WKM: Barycenter-based Wasserstein K -means. n : total number of distributions.

n	W-SDP	D-WKM	B-WKM	Frequency of $\Delta_1 > \Delta_2$
101	1.00	0.82	0.40	0.32
202	1.00	0.84	0.34	0.26
303	1.00	0.72	0.46	0.20

4.2 Gaussian distributions

Next, we simulate random Gaussian measures from model (18) with $K = 4$ and all cluster size equal. We set the centers of each cluster of Gaussians such that all pairwise distances among the barycenters are all equal, i.e., $W_2^2(N(0, V^{(k_1)}), N(0, V^{(k_2)})) \equiv D$ for all $k_1, k_2 \in \{1, 2, 3, 4\}$ with $\mathcal{V} = \max_k \|V^{(k)}\|_{\text{op}} \in [4.5, 5.5]$. We fix the dimension $p = 10$ and vary the sample size $n = 200, 400, 600$. And we set the perturbation parameter $t = 10^{-3}$ on the covariance matrix. The simulation results are reported over 100 times in each setting. Fig. 4 shows the misclassification rate (log-scale) versus the squared distance D between centers. We observe that when the distance between centers of clusters are larger than certain threshold (squared distance $D > 10^{-3}$ in this case), then Wasserstein SDP can achieve exact recovery for different n , while the misclassification rate for the two Wasserstein K -means are stably around 10%. And when the distance between centers of clusters are relatively small, the two Wasserstein K -means and SDP behave similarly.

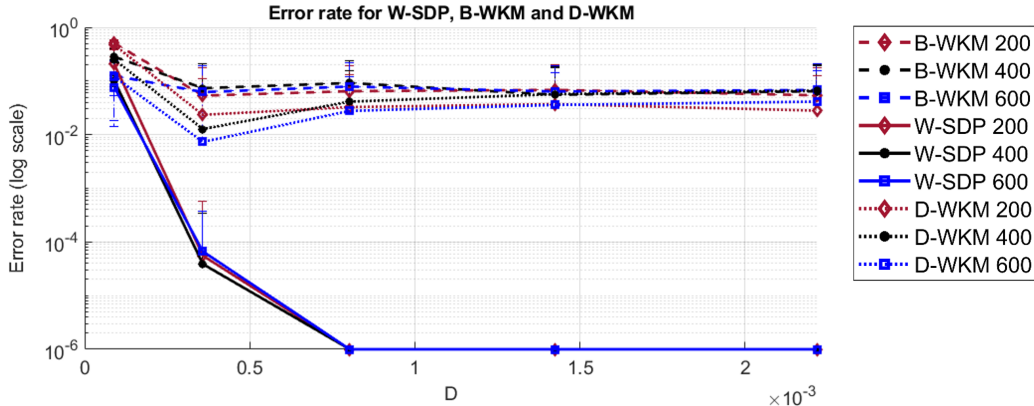


Figure 4: Mis-classification error versus squared distance D from Wasserstein SDP (W-SDP) and barycenter/distance-based Wasserstein K -means (B-WKM and D-WKM) for clustering Gaussians under $n \in \{200, 400, 600\}$. Due to the log-scale, 10^{-6} corresponds to exact recovery.

4.3 Real-data applications

We consider three benchmark image datasets: MNIST, Fashion-MNIST and USPS handwriting digits. Due to complexity issues, we consider subsets of the whole datasets and randomly choose fixed number of images from each clusters based on 10 replicates for each cases. Here we used Sinkhorn divergence to calculate the Wasserstein distance and the Bregman projection with 100 iterations for computing the barycenters, which is efficient and stable for non-degenerate case in practice. For both Wasserstein K -means methods, we use the initialization method in analogue to the K -means++ for Euclidean data, i.e., the first cluster barycenter is chosen uniformly at random as one of the distributions, after which each subsequent cluster barycenter is

chosen from the remaining distributions with probability proportional to its squared Sinkhorn divergence from the distribution’s closest existing cluster barycenter. Codes using MATLAB and Python implementing W-SDP and D-WKM are available at: <https://github.com/Yubo02/Wasserstein-K-means-for-clustering-probability-distributions>.

For MNIST dataset, we choose and fix two clusters: G_1^* containing the number "0" and G_2^* containing the number "5" for two cases. (1) In Case 1, we randomly draw 200 number "0" and 100 number of "5" for each repetition. (2) In Case 2, we double the number and randomly draw 400 number "0" and 200 number of "5" instead. For Fashion-MNIST and USPS handwriting digits dataset, we consider $K = 3$: G_1^* containing the "T-shirt/top" (or the number "0" for USPS handwriting), G_2^* containing the "Trouser" (or the number "5" for USPS handwriting) and G_3^* containing the "Dress" (or the number "7" for USPS handwriting). The cluster sizes are unbalanced where we randomly choose 200, 100 and 100 number from G_1^* , G_2^* and G_3^* respectively. The error rates are shown in Table 2. Detailed setups and more results about F_1 scores (analogous to error rates) as well as time costs are placed at Appendix A due to space limit.

From Table 2, we can observe that the performances for Wasserstein SDP (W-SDP) and distance-based Wasserstein K -means (D-WKM) are better compared with barycenter-based Wasserstein K -means (B-WKM) for all cases. And the results from Table 3 in Appendix A by using F_1 score are consistent with the results from Table 2. The original K -means method behaves similar as barycenter-based Wasserstein K -means in some cases and behaves less preferable for cases such as our experiment on USPS handwriting digits. In particular, the visualization of the clustering results for case 1 has been shown in Fig. 3. From this figure we can find that the classification criterion for B-WKM will end up with the closeness to certain shape of "0", which is characterized by certain angle or the degree of stretch. And this will lead to the high misclassification error for barycenter-based or centroid-based Wasserstein K -means.

Table 2: Error rate (SD) for clustering three benchmark datasets: MNIST, Fashion-MNIST and USPS handwriting digits. MNIST₁ (MNIST₂) refers to the results of Case 1 (Case 2) for MNIST dataset.

	W-SDP	D-WKM	B-WKM	KM
MNIST ₁	0.235 (0.045)	0.156 (0.057)	0.310 (0.069)	0.295 (0.066)
MNIST ₂	0.279 (0.050)	0.185 (0.097)	0.324 (0.032)	0.362 (0.033)
Fashion-MNIST	0.082 (0.020)	0.056 (0.014)	0.141 (0.059)	0.138 (0.099)
USPS handwriting	0.206 (0.020)	0.159 (0.061)	0.240 (0.045)	0.284 (0.025)

5 Discussion

In this paper, we observed and analyzed the peculiar behaviors of Wasserstein barycenters and their results in clustering probability distributions. After that, we proposed the distance-based K-means approach (D-WKW) and its semidefinite program relaxation (W-SDP) by showing the exact recovery results for Gaussians theoretically and numerically. For several real benchmark datasets, we showed results where D-WKM and W-SDP could outperform barycenter-based K-means approach (B-WKM). And we focused on one unbalanced case of two clusters from MNIST and analyzed its behavior through visualization of misclassification for the barycenter-based Wasserstein K -means. The corresponding time costs for B-WKM, D-WKM and W-SDP for benchmark datasets suggest that the scalability for them and especially our approaches could be serious when sample size is large. One of our future goals would be addressing the corresponding computational complexity issues for real data. Another goal is to find out more conclusive results where our approaches are preferable within or out of the realm of unbalanced clusters for real datasets.

Acknowledgments and Disclosure of Funding

Xiaohui Chen was partially supported by NSF CAREER grant DMS-1752614. Yun Yang was partially supported by NSF grant DMS-2210717.

References

- Radoslaw Adamczak. A tail inequality for suprema of unbounded empirical processes with applications to Markov chains. *Electronic Journal of Probability*, 13(none):1000 – 1034, 2008. doi: 10.1214/EJP.v13-521. URL <https://doi.org/10.1214/EJP.v13-521>.
- Martial Agueh and Guillaume Carlier. Barycenters in the wasserstein space. *SIAM J. Math. Anal.*, 43(2):904–924, 2011.
- Daniel Aloise, Amit Deshpande, Pierre Hansen, and Preyas Popat. Np-hardness of euclidean sum-of-squares clustering. *Machine learning*, 75(2):245–248, 2009.
- Luigi Ambrosio, Nicola Gigli, and Giuseppe Savaré. *Gradient flows: in metric spaces and in the space of probability measures*. Springer Science & Business Media, 2005.
- Jean-David Benamou, Guillaume Carlier, Marco Cuturi, Luca Nenna, and Gabriel Peyré. Iterative bregman projections for regularized transportation problems. *SIAM Journal on Scientific Computing*, 37(2):A1111–A1138, 2015.
- Rajendra Bhatia, Tanvi Jain, and Yongdo Lim. On the bures–wasserstein distance between positive definite matrices. *Expositiones Mathematicae*, 37(2):165–191, 2019. ISSN 0723-0869. doi: <https://doi.org/10.1016/j.exmath.2018.01.002>. URL <https://www.sciencedirect.com/science/article/pii/S0723086918300021>.
- Jérémy Bigot, Raúl Gouet, Thierry Klein, and Alfredo López. Geodesic PCA in the Wasserstein space by convex PCA. *Annales de l’Institut Henri Poincaré, Probabilités et Statistiques*, 53(1):1 – 26, 2017. doi: 10.1214/15-AIHP706. URL <https://doi.org/10.1214/15-AIHP706>.
- Yann Brenier. Polar factorization and monotone rearrangement of vector-valued functions. *Communications on Pure and Applied Mathematics*, 44(4):375–417, 1991. doi: <https://doi.org/10.1002/cpa.3160440402>. URL <https://onlinelibrary.wiley.com/doi/abs/10.1002/cpa.3160440402>.
- Samuel Burer and Renato D. C. Monteiro. A nonlinear programming algorithm for solving semidefinite programs via low-rank factorization. *Mathematical Programming*, 95(2):329–357, 2003. doi: 10.1007/s10107-002-0352-8. URL <https://doi.org/10.1007/s10107-002-0352-8>.
- Elsa Cazelles, Vivien Seguy, Jérémy Bigot, Marco Cuturi, and Nicolas Papadakis. Geodesic pca versus log-pca of histograms in the wasserstein space. *SIAM Journal on Scientific Computing*, 40(2):B429–B456, 2018. doi: 10.1137/17M1143459. URL <https://doi.org/10.1137/17M1143459>.
- Frédéric Chazal, Clément Levrard, and Martin Royer. Clustering of measures via mean measure quantization. *Electronic Journal of Statistics*, 15(1):2060 – 2104, 2021. doi: 10.1214/21-EJS1834. URL <https://doi.org/10.1214/21-EJS1834>.
- Xiaohui Chen and Yun Yang. Cutoff for exact recovery of gaussian mixture models. *IEEE Transactions on Information Theory*, 67(6):4223–4238, 2021.
- Yaqing Chen, Zhenhua Lin, and Hans-Georg Müller. Wasserstein regression. *Journal of the American Statistical Association*, 0(0):1–14, 2021. doi: 10.1080/01621459.2021.1956937. URL <https://doi.org/10.1080/01621459.2021.1956937>.
- Pierre Del Moral and Angele Niclas. A taylor expansion of the square root matrix functional, 2017. URL <https://arxiv.org/abs/1705.08561>.
- G. Domazakis, Dimosthenis Drivaliaris, Sotirios Koukoulas, G. I. Papayiannis, Andrianos E. Tsekrekos, and Athanasios N. Yannacopoulos. Clustering measure-valued data with wasserstein barycenters. *arXiv: Machine Learning*, 2019.
- Darina Dvinskikh and Daniil Tiapkin. Improved complexity bounds in wasserstein barycenter problem, 2020. URL <https://arxiv.org/abs/2010.04677>.
- Yingjie Fei and Yudong Chen. Hidden integrality of sdp relaxation for sub-gaussian mixture models. *arXiv:1803.06510*, 2018.

- Aude Genevay, Gabriel Peyre, and Marco Cuturi. Learning generative models with sinkhorn divergences. In Amos Storkey and Fernando Perez-Cruz, editors, *Proceedings of the Twenty-First International Conference on Artificial Intelligence and Statistics*, volume 84 of *Proceedings of Machine Learning Research*, pages 1608–1617. PMLR, 09–11 Apr 2018. URL <https://proceedings.mlr.press/v84/genevay18a.html>.
- Christophe Giraud and Nicolas Verzelen. Partial recovery bounds for clustering with the relaxed k means. *arXiv:1807.07547*, 2018.
- Jan-Christian Hütter and Philippe Rigollet. Minimax estimation of smooth optimal transport maps, 2019. URL <https://arxiv.org/abs/1905.05828>.
- Hicham Janati, Marco Cuturi, and Alexandre Gramfort. Debiased Sinkhorn barycenters. In Hal Daumé III and Aarti Singh, editors, *Proceedings of the 37th International Conference on Machine Learning*, volume 119 of *Proceedings of Machine Learning Research*, pages 4692–4701. PMLR, 13–18 Jul 2020. URL <https://proceedings.mlr.press/v119/janati20a.html>.
- Young-Heon Kim and Brendan Pass. Wasserstein barycenters over riemannian manifolds. *Advances in Mathematics*, 307:640–683, 2017. ISSN 0001-8708. doi: <https://doi.org/10.1016/j.aim.2016.11.026>. URL <https://www.sciencedirect.com/science/article/pii/S0001870815304643>.
- Khang Le, Huy Nguyen, Quang M Nguyen, Tung Pham, Hung Bui, and Nhat Ho. On robust optimal transport: Computational complexity and barycenter computation. In M. Ranzato, A. Beygelzimer, Y. Dauphin, P.S. Liang, and J. Wortman Vaughan, editors, *Advances in Neural Information Processing Systems*, volume 34, pages 21947–21959. Curran Associates, Inc., 2021. URL <https://proceedings.neurips.cc/paper/2021/file/b80ba73857eed2a36dc7640e2310055a-Paper.pdf>.
- Stuart Lloyd. Least squares quantization in pcm. *IEEE Transactions on Information Theory*, 28: 129–137, 1982.
- John Lott. Some geometric calculations on wasserstein space. *Communications in Mathematical Physics*, 277(2):423–437, 2008. doi: 10.1007/s00220-007-0367-3. URL <https://doi.org/10.1007/s00220-007-0367-3>.
- Yu Lu and Harrison Zhou. Statistical and computational guarantees of lloyd’s algorithm and its variants. *arXiv:1612.02099*, 2016.
- J.B. MacQueen. Some methods for classification and analysis of multivariate observations. *Proc. Fifth Berkeley Sympos. Math. Statist. and Probability*, pages 281–297, 1967.
- Robert J. McCann. A convexity principle for interacting gases. *Advances in Mathematics*, 128(1): 153–179, 1997. ISSN 0001-8708. doi: <https://doi.org/10.1006/aima.1997.1634>. URL <https://www.sciencedirect.com/science/article/pii/S0001870897916340>.
- Marina Meila and Jianbo Shi. Learning segmentation by random walks. In *In Advances in Neural Information Processing Systems*, pages 873–879. MIT Press, 2001.
- Andrew Y. Ng, Michael I. Jordan, and Yair Weiss. On spectral clustering: Analysis and an algorithm. In *Advances in Neural Information Processing Systems*, pages 849–856. MIT Press, 2001.
- Jiming Peng and Yu Wei. Approximating k -means-type clustering via semidefinite programming. *SIAM J. OPTIM*, 18(1):186–205, 2007.
- Philippe Rigollet and Jonathan Weed. Uncoupled isotonic regression via minimum Wasserstein deconvolution. *Information and Inference: A Journal of the IMA*, 8(4):691–717, 04 2019. ISSN 2049-8772. doi: 10.1093/imaiai/iaz006. URL <https://doi.org/10.1093/imaiai/iaz006>.
- Filippo Santambrogio and Xu-Jia Wang. Convexity of the support of the displacement interpolation: Counterexamples. *Applied Mathematics Letters*, 58:152–158, 2016. ISSN 0893-9659. doi: <https://doi.org/10.1016/j.aml.2016.02.016>. URL <https://www.sciencedirect.com/science/article/pii/S0893965916300726>.

- Vivien Seguy and Marco Cuturi. Principal geodesic analysis for probability measures under the optimal transport metric. In C. Cortes, N. Lawrence, D. Lee, M. Sugiyama, and R. Garnett, editors, *Advances in Neural Information Processing Systems*, volume 28. Curran Associates, Inc., 2015. URL <https://proceedings.neurips.cc/paper/2015/file/f26dab9bf6a137c3b6782e562794c2f2-Paper.pdf>.
- Justin Solomon, Fernando de Goes, Gabriel Peyré, Marco Cuturi, Adrian Butscher, Andy Nguyen, Tao Du, and Leonidas Guibas. Convolutional wasserstein distances: Efficient optimal transportation on geometric domains. *ACM Trans. Graph.*, 34(4), jul 2015. ISSN 0730-0301. doi: 10.1145/2766963. URL <https://doi.org/10.1145/2766963>.
- Aad W. van der Vaart and Jon A. Wellner. *Maximal Inequalities and Covering Numbers*, pages 95–106. Springer New York, New York, NY, 1996. ISBN 978-1-4757-2545-2. doi: 10.1007/978-1-4757-2545-2_14. URL https://doi.org/10.1007/978-1-4757-2545-2_14.
- Santosh Vempala and Grant Wang. A spectral algorithm for learning mixture models. *J. Comput. Syst. Sci.*, 68:2004, 2004.
- Isabella Verdinelli and Larry Wasserman. Hybrid Wasserstein distance and fast distribution clustering. *Electronic Journal of Statistics*, 13(2):5088 – 5119, 2019. doi: 10.1214/19-EJS1639. URL <https://doi.org/10.1214/19-EJS1639>.
- Roman Vershynin. *High-Dimensional Probability: An Introduction with Applications in Data Science*. Cambridge Series in Statistical and Probabilistic Mathematics. Cambridge University Press, 2018. doi: 10.1017/9781108231596.
- Cédric Villani. *Topics in optimal transportation*. Graduate studies in mathematics. American mathematical society, 2003.
- Ulrike von Luxburg. A tutorial on spectral clustering. *Statistics and Computing*, 17(4):395–416, 2007.
- Ulrike von Luxburg, Mikhail Belkin, and Olivier Bousquet. Consistency of spectral clustering. *Annals of Statistics*, 36(2):555–586, 2008.
- Yubo Zhuang, Xiaohui Chen, and Yun Yang. Sketch-and-lift: scalable subsampled semidefinite program for k-means clustering. In Gustau Camps-Valls, Francisco J. R. Ruiz, and Isabel Valera, editors, *Proceedings of The 25th International Conference on Artificial Intelligence and Statistics*, volume 151 of *Proceedings of Machine Learning Research*, pages 9214–9246. PMLR, 28–30 Mar 2022. URL <https://proceedings.mlr.press/v151/zhuang22a.html>.

A Additional details on application for real datasets in Section 4.3

In this section, we provide more details of setups and results for real applications in Section 4.3. The results of error rates, F_1 scores and time costs are shown in Table 2, Table 3 and Table 4 respectively, which are based on 10 replicates.¹

Table 3: F_1 score (SD) for clustering three benchmark datasets: MNIST, Fashion-MNIST and USPS handwriting digits. MNIST₁ (MNIST₂) refers to the results of Case 1 (Case 2) for MNIST dataset.

	W-SDP	D-WKM	B-WKM	KM
MNIST ₁	0.771 (0.044)	0.842 (0.056)	0.698 (0.067)	0.708 (0.063)
MNIST ₂	0.729 (0.049)	0.814 (0.093)	0.685 (0.031)	0.647 (0.032)
Fashion-MNIST	0.919 (0.018)	0.934 (0.036)	0.817 (0.117)	0.791(0.168)
USPS handwriting	0.799 (0.019)	0.835 (0.081)	0.761 (0.060)	0.689 (0.093)

Table 4: Time cost (SD) for clustering three benchmark datasets: MNIST, Fashion-MNIST and USPS handwriting digits. MNIST₁ (MNIST₂) refers to the results of Case 1 (Case 2) for MNIST dataset.

	W-SDP	D-WKM	B-WKM	KM
MNIST ₁	525.13 (4.70)	524.80 (4.92)	388.87 (647.15)	0.01 (0.01)
MNIST ₂	2187.66 (74.67)	2160.91 (7.26)	693.67 (142.57)	0.02 (0.00)
Fashion-MNIST	849.24 (7.09)	852.49 (8.60)	463.28 (176.32)	0.01 (0.00)
USPS handwriting	1100.87 (19.13)	1098.05 (16.41)	317.12 (113.94)	0.02 (0.01)

First we run our Wasserstein SDP algorithm against Wasserstein K -means on the MNIST dataset for two cases. (1) For the first case, we choose two clusters: G_1^* containing the number "0" and G_2^* containing the number "5", so that the number of clusters is $K = 2$ in the algorithms. The cluster sizes are unbalanced with $|G_1^*|/|G_2^*| = 2$, where we randomly choose 200 number "0" and 100 number of "5" for each repetition. (2) For the second case, we follow the same settings as case 1 except that randomly choose 400 number "0" and 200 number of "5" for each repetition.

Next we considered benchmark dataset Fashion-MNIST 28×28 containing 10 clusters of 28×28 greyscale images of clothes. Here we choose three clusters: G_1 containing the "T-shirt/top", G_2 containing the "Trouser" and G_3 containing the "Dress", so that the number of clusters is $K = 3$ in the algorithms. The cluster sizes are unbalanced where we randomly choose 200, 100 and 100 number from G_1 , G_2 and G_3 respectively for each repetition.

Finally, we consider the USPS handwriting dataset, analogous to MNIST, which contains digits automatically scanned from envelopes by the U.S. Postal Service containing a total of 9,298 16×16 pixel grayscale samples. We choose three clusters: G_1 containing the number "0", G_2 containing the number "5" and G_3 containing the number "7", so that the number of clusters is $K = 3$ in the algorithms. The cluster sizes are unbalanced where we randomly choose 200, 100 and 100 number from G_1 , G_2 and G_3 respectively for each repetition.

Now if we look at the time cost for two cases on MNIST (MNIST₁ and MNIST₂) in Table 4, we can see that Wasserstein SDP (W-SDP), distance-based Wasserstein K -means (D-WKM) and barycenter-based Wasserstein K -means (B-WKM) all have time complexity issues when we enlarge n . The large variance for B-WKM for MNIST₁ is due to the convergence of the algorithm. The total iterations for B-WKM in case 1 achieves maximum iteration 100 for 1 replicate out of 10 total replicates. More arguments for time complexity can be found in Appendix B.

B Additional details on simulation studies in Section 4.1

In this section, we provide more details of our simulation setups and results for Gaussian mixtures in Section 4.1.

¹We run all the simulations and experiments except for USPS datasets on the machine with Intel Core i7-10700K 3.80 GHz 64 bit 8-core 16 Tread Processor and 16 GB DDR4 Memory; run experiments on USPS datasets with 1.6 GHz Dual-Core Intel Core i5 and 8 GB 2133 MHz LPDDR3 Memory.

We set $m_1 = 40 \cdot r$, $m_2 = r$, $m_3 = 20 \cdot r$ which means that there are total $81 \cdot r$ number of distributions in G_1 , $20 \cdot r$ distributions in G_2 . The r is set to be 1, 2, 3, where we have $n = 101, 202, 303$ respectively. The mean for the Gaussian distributions are shown in the table below. The entries of covariance matrices for the Gaussian distributions are chosen to be $O(10^{-3})$ for μ_1, μ_2 and they are chosen to be $O(10^{-6})$ for μ_3 and μ_4 . Then we scale down the distribution with scaling parameter equals 0.5. This ensures that with high probability, all the distributions will fall into the bounded range $[0, 1] \times [0, 1]$.

The algorithm we use to get the barycenter is Frank-Wolfe algorithm with 200 iterations. And we use Sinkhorn divergence to calculate the Wasserstein distance. The regularization parameters for both algorithms are chosen to be 10^{-3} . To approximate the true distribution, first we divide $[0, 1] \times [0, 1]$ range into 80×80 grids, then we randomly sample 600 samples each time and count the number of times it falls into certain grid to approximate the distribution. The results show us that for each n and each iterations among 50 repetitions, all the distributions in G_2^* will be assigned to same cluster, so it will be reasonable to define that μ_3 is misclassified if any copy of them are in the same cluster of an arbitrarily chosen μ from G_2^* .

The arrangement of mean for Gaussian mixture models shown in Table 5 indicates that the distributions are set based on Example 3. Recall that in Section 4.1, $\Delta_* := \max_{k=1,2} \max_{i,j \in G_k} W_2(\mu_i, \mu_j)$ and $\Delta^* := \min_{i \in G_1, j \in G_2} W_2(\mu_i, \mu_j)$ are the maximum within-cluster distance and the minimum between-cluster distance respectively. Table 7 shows that $\Delta_* < \Delta^*$ on average and $\Delta_* < \Delta^*$ for around 80% among 50 repetitions. So we can expect Wasserstein SDP to correctly cluster all data points in the Wasserstein space. From Table 6 we can observe that in our settings the time cost for Wasserstein SDP and distance-based Wasserstein K -means is relatively lower than the time cost for barycenter-based Wasserstein K -means. But we can see that as n increases, the time cost for B-WKM grows almost linearly w.r.t. n while almost quadratically for W-SDP and D-WKM. Thus we should expect relatively higher time cost for W-SDP and D-WKM when n is sufficiently large, where we can consider several methods to bring down the time cost (e.g., subsampling-based method for SDP from Zhuang et al. [2022]).

Computationally speaking, the calculations of Wasserstein distances and barycenters are usually based on one-step discretization and one-step application of entropic regularization methods such as Sinkhorn (Genevay et al. [2018], Janati et al. [2020]). Dvinskikh and Tiapkin [2020] shows that the complexity of calculating barycenters should be of the order $O(nd^2/\epsilon^2)$ or $O(ng^4/\epsilon^2)$, where n is the total number of distributions, $d = g^2$ is the discretization size, e.g. $g = 28$ for MNIST datasets and ϵ is the numerical accuracy; while Le et al. [2021] gives a $O(d^2/\epsilon)$ or $O(g^4/\epsilon)$ complexity algorithm for calculating the Wasserstein distance on robust optimal transport.

Table 5: Positions $(x, y) \in \mathbb{R}^2$ of means for two-dimensional mixture of Gaussian distributions for the counter example in Section 4.1.

	$a_{1,1}$	$a_{1,2}$	$a_{2,1}$	$a_{2,2}$	$a_{3,1}$	$a_{3,2}$	$a_{4,1}$	$a_{4,2}$
x	0.75	0.25	0.75	0.25	0.9	0.9	1.3	1.3
y	1.15	0.85	0.85	1.15	0.85	1.15	0.75	1.25

Table 6: The time cost with standard deviation shown in parentheses for the counter example. TC: Time cost, W-SDP: Wasserstein SDP, D-WKM: Distance-based Wasserstein K -means, B-WKM: Barycenter-based Wasserstein K -means.

n	TC for W-SDP (SD)	TC for D-WKM	TC for B-WKM (SD)
101	14.50 (0.5873)	14.15 (0.5132)	181.1 (372.4)
202	56.94 (1.490)	54.98 (1.516)	341.0 (136.2)
303	128.4 (3.640)	123.9 (3.606)	549.2 (200.2)

C Background on optimal transport

The optimal transport (OT) problem (a.k.a. the Monge problem) is to find an optimal map $T^* : \mathbb{R}^p \rightarrow \mathbb{R}^p$ for transporting a source distribution μ_0 to a target distribution μ_1 that minimizes some cost

Table 7: Estimated Wasserstein distances with standard deviation shown in parentheses and frequency of $\Delta^* > \Delta_*$ for the counter example.

n	Δ_*	Δ^*	Frequency of $\Delta_* < \Delta^*$
101	0.1978 (0.0055)	0.2046 (0.0050)	0.8200
202	0.1990 (0.0058)	0.2050 (0.0051)	0.8200
303	0.1996 (0.0067)	0.2052 (0.0050)	0.7600

function $c : \mathbb{R}^p \times \mathbb{R}^p \rightarrow \mathbb{R}$:

$$\min_{T: \mathbb{R}^p \rightarrow \mathbb{R}^p} \left\{ \int_{\mathbb{R}^p} c(x, T(x)) d\mu_0(x) : T_{\#}\mu_0 = \mu_1 \right\}, \quad (20)$$

where $T_{\#}\mu$ denotes the pushforward measure defined by $(T_{\#}\mu)(B) = \mu(T^{-1}(B))$ for measurable subset $B \subset \mathbb{R}^p$. A standard example of the cost function is the quadratic cost $c(x, y) = \|x - y\|_2^2$. The Monge problem (20) with the quadratic cost induces a metric, known as the *2-Wasserstein distance*, on the space $\mathcal{P}_2(\mathbb{R}^p)$ of probability measures on \mathbb{R}^p with finite second moments. In particular, the 2-Wasserstein distance can be expressed in the relaxed Kantorovich form:

$$W_2^2(\mu_0, \mu_1) := \min_{\gamma} \left\{ \int_{\mathbb{R}^p \times \mathbb{R}^p} \|x - y\|_2^2 d\gamma(x, y) \right\}, \quad (21)$$

where minimization over γ runs over all possible couplings with marginals μ_0 and μ_1 [Villani, 2003]. It is well-known from Brenier's theorem [Brenier, 1991] that if the source measure μ_0 does not charge on small subsets of \mathbb{R}^p (i.e., subsets of Hausdorff dimension at most $p - 1$), then there exists a unique μ_0 -almost everywhere OT map T^* solving (20). That is, $T_{\#}^*\mu_0 = \mu_1$ and

$$W_2^2(\mu_0, \mu_1) = \int_{\mathbb{R}^p} \|x - T^*(x)\|_2^2 d\mu_0(x).$$

Let $(\mu_t)_{t=0}^1$ be the constant-speed geodesic connecting $\mu_0, \mu_1 \in \mathcal{P}_2(\mathbb{R}^p)$. Then for any $\nu \in \mathcal{P}_2(\mathbb{R}^p)$ and $t \in [0, 1]$, we have

$$W_2^2(\mu_t, \nu) \geq (1 - t)W_2^2(\mu_0, \nu) + tW_2^2(\mu_1, \nu) - t(1 - t)W_2^2(\mu_0, \mu_1). \quad (22)$$

The above semiconcavity inequality (22) can be interpreted as that the Wasserstein space $\mathcal{P}_2(\mathbb{R}^p)$ is a *positive curved* metric space (PC-space) in the sense of Alexandrov (cf. Section 7.3 and Section 12.3 in Ambrosio et al. [2005]).

D Additional proofs

In this section, we will give detailed proofs for Example 1, Lemma 4 and Theorem 8. For the proof of Theorem 8, we will first introduce the main part and put the rest proofs of corresponding lemmas at the end of this section to make it clear.

D.1 Proof of Example 1

Recall that $\mu_0(s) = (1 - s)/2$ and $\mu_1(s) = (1 + s)/2$ are probability densities supported on the line segments $L_0 = \{(s, as) : s \in [-1, 1]\}$ and $L_1 = \{(s, -as) : s \in [-1, 1]\}$ for some $a \in (0, 1)$, respectively. To derive the optimal transport (OT) map T from μ_0 to μ_1 , it suffices to consider the one-dimensional OT problem by parameterization of $T : [-1, 1] \rightarrow [-1, 1]$ identified via $(s, as) \mapsto (T(s), -aT(s))$. Then our goal is to find the solution to the following optimization problem

$$\begin{aligned} & \min_{T: T_{\#}\mu_0 = \mu_1} \int_{-1}^1 \|(s, -as) - (T(s), -aT(s))\|_2^2 d\mu_0(s) \\ &= \min_{T: T_{\#}\mu_0 = \mu_1} \int_{-1}^1 [(s - T(s))^2 + a^2(s + T(s))^2] d\mu_0(s) \\ &= (1 - a^2) \times \min_{T: T_{\#}\mu_0 = \mu_1} \int_{-1}^1 \left[\sqrt{\frac{1 + a^2}{1 - a^2}} T(s) - s \right]^2 d\mu_0(s) + \text{constant}, \end{aligned}$$

where the constant does not depend on T . Now rescale the distribution density μ_1 to

$$\tilde{\mu}_1(s) = \sqrt{\frac{1-a^2}{1+a^2}} \mu_1 \left(\sqrt{\frac{1-a^2}{1+a^2}} s \right) \quad \text{for } s \in \left[-\sqrt{\frac{1+a^2}{1-a^2}}, \sqrt{\frac{1+a^2}{1-a^2}} \right],$$

and define the transport map $\tilde{T} = \sqrt{\frac{1+a^2}{1-a^2}} T$ on $[-1, 1]$. To find the OT map T such that $T_{\#}\mu_0 = \mu_1$, it suffices to find the OT map \tilde{T} such that $\tilde{T}_{\#}\mu_0 = \tilde{\mu}_1$, i.e.,

$$\min_{\tilde{T}: \tilde{T}_{\#}\mu_0 = \tilde{\mu}_1} \int_{-1}^1 [\tilde{T}(s) - s]^2 d\mu_0(s),$$

whose solution is known as the *quantile transform* for one-dimensional distributions. Specifically, let

$$F_0(s) = \int_{-1}^s \mu_0(t) dt = \frac{1}{2} \left(s - \frac{1}{2}s^2 + \frac{3}{2} \right) \quad \text{for } s \in [-1, 1],$$

be the cumulative distribution function (cdf) of the density μ_0 and

$$\tilde{F}_1(s) = \int_{-\sqrt{\frac{1+a^2}{1-a^2}}}^s \tilde{\mu}_1(t) dt = \frac{1}{2} \left(\sqrt{\frac{1-a^2}{1+a^2}} s + \frac{1}{2} \cdot \frac{1-a^2}{1+a^2} s^2 + \frac{1}{2} \right) \quad \text{for } s \in \left[-\sqrt{\frac{1+a^2}{1-a^2}}, \sqrt{\frac{1+a^2}{1-a^2}} \right],$$

be the cdf of the density $\tilde{\mu}_1$. It is easy to find that

$$\tilde{F}_1^{-1}(y) = \sqrt{\frac{1+a^2}{1-a^2}} (\sqrt{4y} - 1) \quad \text{for } y \in [0, 1].$$

Then the OT map \tilde{T} from μ_0 to $\tilde{\mu}_1$ is given by

$$\tilde{T}(s) = \tilde{F}_1^{-1} \circ F_0(s) = \sqrt{\frac{1+a^2}{1-a^2}} [-1 + \sqrt{4 - (1-s)^2}], \quad s \in [-1, 1].$$

This gives the OT map T from μ_0 to μ_1 (in the one-dimensional parameterization form) as

$$T(s) = -1 + \sqrt{4 - (1-s)^2}. \quad (23)$$

Thus, the OT map T from μ_0 to μ_1 as (degenerate) probability distribution in \mathbb{R}^2 is given by

$$T(s, as) = (-1 + \sqrt{4 - (1-s)^2}, -a \cdot (-1 + \sqrt{4 - (1-s)^2})).$$

D.2 Proof of Lemma 4 in Section 2.1

Recall the settings as following

$$\begin{aligned} \mu_1 &= 0.5 \delta_{(x,y)} + 0.5 \delta_{(-x,-y)}, & \mu_2 &= 0.5 \delta_{(x,-y)} + 0.5 \delta_{(-x,y)}, \\ \mu_3 &= 0.5 \delta_{(x+\epsilon_1,y)} + 0.5 \delta_{(x+\epsilon_1,-y)}, & \text{and } \mu_4 &= 0.5 \delta_{(x+\epsilon_1+\epsilon_2,y)} + 0.5 \delta_{(x+\epsilon_1+\epsilon_2,-y)}, \end{aligned}$$

where $\delta_{(x,y)}$ denotes the point mass measure at point $(x, y) \in \mathbb{R}^2$, and $(x, y, \epsilon_1, \epsilon_2)$ are positive constants.

Lemma 4 (Configuration characterization). If $(x, y, \epsilon_1, \epsilon_2)$ satisfies

$$y^2 < \min\{x^2, 0.25 \Delta_{\epsilon_1, x}\} \quad \text{and} \quad \Delta_{\epsilon_1, x} < \epsilon_2^2 < \Delta_{\epsilon_1, x} + y^2,$$

where $\Delta_{\epsilon_1, x} := \epsilon_1^2 + 2x^2 + 2x\epsilon_1$, then for all sufficiently large m (number of copies of μ_1 and μ_2),

$$W_2(\mu_3, \mu_2^*) < W_2(\mu_3, \mu_1^*) \quad \text{and} \quad \underbrace{\max_{k=1,2} \max_{i,j \in G_k} W_2(\mu_i, \mu_j)}_{\text{largest within-cluster distance}} < \underbrace{\min_{i \in G_1, j \in G_2} W_2(\mu_i, \mu_j)}_{\text{least between-cluster distance}},$$

where μ_k^* denotes the Wasserstein barycenter of cluster G_k for $k = 1, 2$.

Proof. For any $w_i \in \mathbb{R}^2, i = 1, 2, 3, 4$, let $\mu = 0.5 \delta_{w_1} + 0.5 \delta_{w_2}$, $\nu = 0.5 \delta_{w_3} + 0.5 \delta_{w_4}$. By definition of Wasserstein distance we can show that

$$W_2^2(\mu, \nu) = 0.5 \min\{\|w_1 - w_3\|^2 + \|w_2 - w_4\|^2, \|w_1 - w_4\|^2 + \|w_2 - w_3\|^2\}.$$

Let $\mu_0 = 0.5 \delta_{(x,0)} + 0.5 \delta_{(-x,0)}$, by algebraic calculation it is direct to check

$$W_2(\mu_3, \mu_2^*) < W_2(\mu_3, \mu_0) \quad \text{and} \quad \underbrace{\max_{k=1,2} \max_{i,j \in G_k} W_2(\mu_i, \mu_j)}_{\text{largest within-cluster distance}} < \underbrace{\min_{i \in G_1, j \in G_2} W_2(\mu_i, \mu_j)}_{\text{least between-cluster distance}}$$

once plugging in the assumptions. So we only need to show that $\forall \varepsilon, \exists M$, s.t. when $m > M$ we have $W_2^2(\mu_3, \mu_1^*) \geq W_2^2(\mu_3, \mu_0) - \varepsilon$. For notation simplicity, let $v_x = (x, 0), v_{-x} = (-x, 0), v_1 = (x, y), v_2 = (-x, -y), v_3 = (x, -y), v_4 = (x, -y)$. By definition we know there exist measures $\xi_i, i = 1, 2, 3, 4$, s.t.

$$W_2^2(\mu_1^*, \mu_1) = \int \|v - v_1\|^2 d\xi_1(v) + \int \|v - v_2\|^2 d\xi_2(v),$$

$$W_2^2(\mu_1^*, \mu_2) = \int \|v - v_3\|^2 d\xi_3(v) + \int \|v - v_4\|^2 d\xi_4(v),$$

where $\mu_1^* = \xi_1 + \xi_2 = \xi_3 + \xi_4$ with $\xi_i(\mathbb{R}^2) = 0.5, \forall i$. Furthermore, if we define $\xi_{i,j} = \xi_i \cdot \xi_j / \mu_1^*, i \in \{1, 2\}, j \in \{3, 4\}$, then $\xi_i = \xi_{i,3} + \xi_{i,4}, \xi_j = \xi_{1,j} + \xi_{2,j}, i \in \{1, 2\}, j \in \{3, 4\}$. Thus

$$\begin{aligned} W_2^2(\mu_1^*, \mu_1) + W_2^2(\mu_1^*, \mu_2) &= \sum_{i=1}^4 \int \|v - v_i\|^2 d\xi_i(v) \\ &= \sum_{i \in \{1,2\}, j \in \{3,4\}} \int \|v - v_i\|^2 + \|v - v_j\|^2 d\xi_{i,j}(v). \end{aligned}$$

Now suppose $t = \|v - v_x\|$, by algebraic calculation we can get

$$\|v - v_1\|^2 + \|v - v_3\|^2 = t^2 + 2y^2.$$

Choose $T > 0$ s.t. $T^2 < \min\{2x^2 - 2y^2, y^2\}$, then we have

$$\begin{aligned} W_2^2(\mu_1^*, \mu_1) + W_2^2(\mu_1^*, \mu_2) &= \sum_{i \in \{1,2\}, j \in \{3,4\}} \int \|v - v_i\|^2 + \|v - v_j\|^2 d\xi_{i,j}(v) \\ &\leq \int_{B_T(v_x)} \|v - v_1\|^2 + \|v - v_3\|^2 d\xi_{1,3}(v) + \int_{B_T(v_{-x})} \|v - v_2\|^2 + \|v - v_4\|^2 d\xi_{2,4}(v) \\ &\quad + (T^2 + 2y^2)(1 - \xi_{1,3}(B_T(v_x)) - \xi_{2,4}(B_T(v_{-x}))) \\ &= \int_{B_T(v_x)} t_1(v)^2 d\xi_{1,3}(v) + \int_{B_T(v_{-x})} t_2(v)^2 d\xi_{2,4}(v) + 2y^2 + T^2(1 - \xi_{1,3}(B_T(v_x)) - \xi_{2,4}(B_T(v_{-x}))), \end{aligned}$$

where $B_t(v)$ stands for the ball with radius t centered at v , $t_1(v) := \|v - v_x\|, t_2(v) := \|v - v_{-x}\|$. On the other hand, by definition we know that

$$\begin{aligned} &m \cdot W_2^2(\mu_1^*, \mu_1) + m \cdot W_2^2(\mu_1^*, \mu_2) + W_2^2(\mu_1^*, \mu_3) \\ &\leq m \cdot W_2^2(\mu_0, \mu_1) + m \cdot W_2^2(\mu_0, \mu_2) + W_2^2(\mu_0, \mu_3) \\ &= m \cdot (2y^2) + C, \end{aligned}$$

where $C := W_2^2(\mu_0, \mu_3)$. So we have $W_2^2(\mu_1^*, \mu_1) + W_2^2(\mu_1^*, \mu_2) \leq 2y^2 + C/m$. i.e.,

$$\int_{B_T(v_x)} t_1(v)^2 d\xi_{1,3}(v) + \int_{B_T(v_{-x})} t_2(v)^2 d\xi_{2,4}(v) + T^2(1 - \xi_{1,3}(B_T(v_x)) - \xi_{2,4}(B_T(v_{-x}))) \leq \frac{C}{m}.$$

So we have

$$\begin{aligned} \int_{B_T(v_x)} t_1(v)^2 d\xi_{1,3}(v) &\leq \frac{C}{m}, \quad \int_{B_T(v_{-x})} t_2(v)^2 d\xi_{2,4}(v) \leq \frac{C}{m}, \\ 0.5 - \xi_{1,3}(B_T(v_x)) &\leq \frac{C}{T^2 m}, \quad 0.5 - \xi_{2,4}(B_T(v_{-x})) \leq \frac{C}{T^2 m}. \end{aligned}$$

Now suppose $v_{\epsilon_1} := (x + \epsilon_1, y), v_{-\epsilon_1} := (x + \epsilon_1, -y)$, note that $T^2 < y^2 < \epsilon_1^2 + y^2$ and $W_2^2(\mu_3, \mu_0) = 0.5\|v_x - v_{\epsilon_1}\|^2 + 0.5\|v_{-x} - v_{-\epsilon_1}\|^2$. By definition of Wasserstein distance and symmetry we have

$$\begin{aligned} W_2^2(\mu_3, \mu_1^*) &\geq \int_{B_T(v_x)} (\|v_x - v_{\epsilon_1}\| - t_1(v))^2 d\xi_{1,3}(v) + \int_{B_T(v_{-x})} (\|v_{-x} - v_{-\epsilon_1}\| - t_2(v))^2 d\xi_{2,4}(v) \\ &\geq \|v_x - v_{\epsilon_1}\|^2 \xi_{1,3}(B_T(v_x)) + \|v_{-x} - v_{-\epsilon_1}\|^2 \xi_{2,4}(B_T(v_{-x})) \\ &\quad - 2\|v_x - v_{\epsilon_1}\| \int_{B_T(v_x)} t_1(v) d\xi_{1,3}(v) - 2\|v_{-x} - v_{-\epsilon_1}\| \int_{B_T(v_{-x})} t_2(v) d\xi_{2,4}(v) \\ &\geq W_2^2(\mu_3, \mu_0) - C_1^2 \cdot \frac{C}{T^2 m} - C_2^2 \cdot \frac{C}{T^2 m} \\ &\quad - 2C_1 \int_{B_T(v_x)} t_1(v) d\xi_{2,4}(v) - 2C_2 \int_{B_T(v_{-x})} t_2(v) d\xi_{2,4}(v), \end{aligned}$$

where $C_1 = \|v_x - v_{\epsilon_1}\|, C_2 = \|v_{-x} - v_{-\epsilon_1}\|$. Set $\forall \varepsilon > 0$. Finally, by Hölder's inequality we have

$$\begin{aligned} W_2^2(\mu_3, \mu_1^*) &\geq W_2^2(\mu_3, \mu_0) - C_1^2 \cdot \frac{C}{T^2 m} - C_2^2 \cdot \frac{C}{T^2 m} \\ &\quad - 2C_1 \sqrt{\int_{B_T(v_x)} t_1^2(v) d\xi_{2,4}(v)} - 2C_2 \sqrt{\int_{B_T(v_{-x})} t_2^2(v) d\xi_{2,4}(v)} \\ &\geq W_2^2(\mu_3, \mu_0) - C_1^2 \cdot \frac{C}{T^2 m} - C_2^2 \cdot \frac{C}{T^2 m} - 2C_1 \sqrt{\frac{C}{m}} - 2C_2 \sqrt{\frac{C}{m}} \\ &\geq W_2^2(\mu_3, \mu_0) - \varepsilon, \end{aligned}$$

for large m , as desired. \blacksquare

D.3 Proof of Theorem 8 in Section 3

Theorem 8 (Exact recovery for clustering Gaussians). Let $\Delta^2 := \min_{k \neq l} d^2(V^{(k)}, V^{(l)})$ denote the minimal pairwise separation among clusters, $\bar{n} := \max_{k \in [K]} n_k$ (and $\underline{n} := \min_{k \in [K]} n_k$) the maximum (minimum) cluster size, and $m := \min_{k \neq l} \frac{2n_k n_l}{n_k + n_l}$ the minimal pairwise harmonic mean of cluster sizes. Suppose the covariance matrix V_i of Gaussian distribution $\nu_i = N(0, V_i)$ is independently drawn from model (18) for $i = 1, 2, \dots, n$. Let $\beta \in (0, 1)$. If the separation Δ^2 satisfies

$$\Delta^2 > \bar{\Delta}^2 := \frac{C_1 t^2}{\min\{(1 - \beta)^2, \beta^2\}} \mathcal{V} p^2 \log n,$$

then the SDP (17) achieves exact recovery with probability at least $1 - C_2 n^{-1}$, provided that

$$\underline{n} \geq C_3 \log^2 n, \quad t \leq C_4 \sqrt{\log n} / [(p + \log \bar{n}) \mathcal{V}^{1/2} T_v^{1/2}], \quad n/m \leq C_5 \log n,$$

where $\mathcal{V} = \max_k \|V^{(k)}\|_{\text{op}}, T_v = \max_k \text{Tr}[(V^{(k)})^{-1}]$, and $C_i, i = 1, 2, 3, 4, 5$ are constants.

Lemma 10 (Dual argument for SDP (Section B in Chen and Yang [2021])). The sufficient condition for $Z^* = \sum_{k \in [K]} \frac{1}{n_k} 1_{G_k} 1_{G_k}^T$ to be the unique solution of the SDP problem is to find (λ, α, B) s.t.

$$\begin{aligned} (C_1) \quad & B \geq 0 \quad (B_{G_k G_k} = 0, B_{G_k G_l} > 0, \forall k \neq l), \\ (C_2) \quad & W_n := \lambda Id + \frac{1}{2}(1\alpha^T + \alpha 1^T) - A - B \succeq 0, \\ (C_3) \quad & \text{Tr}(W_n Z^*) = 0, \\ (C_4) \quad & \text{Tr}(B Z^*) = 0, \end{aligned}$$

which implies that

$$\alpha_{G_k} = \frac{2}{n_k} A_{G_k G_k} 1_{n_k} - \frac{\lambda}{n_k} 1_{n_k} - \frac{1}{n_k^2} (1_{n_k}^T A_{G_k G_k} 1_{n_k}).$$

$$[B_{G_l G_k} 1_{n_k}]_j = -\frac{n_l + n_k}{2n_l} \lambda + \frac{n_k}{2} \left[\frac{1}{n_l^2} \sum_{s,r \in G_l} d^2(V_s, V_r) - \frac{1}{n_k^2} \sum_{s,r \in G_k} d^2(V_s, V_r) \right] \\ + n_k \left[\frac{1}{n_k} \sum_{r \in G_k} d^2(V_j, V_r) - \frac{1}{n_l} \sum_{r \in G_l} d^2(V_j, V_r) \right],$$

for $k \neq l$, $j \in G_l$.

Remarks. It can be justified that if we can find (λ, B) satisfying above equations, then (C_3) , (C_4) will hold automatically. Details can be found in Section B in Chen and Yang [2021].

Now we will proof the main theorem by two steps. First we will provide a lower bound for $[B_{G_l G_k} 1_{n_k}]_j$. Similar to the argument from Chen and Yang [2021], we want to set λ properly such that (C_1) can hold. In the next step we will try to verify that the choice of (λ, α, B) and the conditions on the signals could actually imply (C_2) . And since number of clusters K is treated as fixed for most practical settings, we will not emphasize $K = O(1)$.

D.3.1 Proof of main result.

Step 1 (Construct (λ, B)). Recall $[B_{G_l G_k} 1_{n_k}]_j = -\frac{n_l + n_k}{2n_l} \lambda + n_k L$, where L equals

$$\frac{1}{2} \left[\frac{1}{n_l^2} \sum_{s,r \in G_l} d^2(V_s, V_r) - \frac{1}{n_k^2} \sum_{s,r \in G_k} d^2(V_s, V_r) \right] + \left[\frac{1}{n_k} \sum_{r \in G_k} d^2(V_j, V_r) - \frac{1}{n_l} \sum_{r \in G_l} d^2(V_j, V_r) \right].$$

For L defined above, by Lemma 14, we have

$$L \geq d^2(V^{(l)}, V^{(k)}) - d(V^{(l)}, V^{(k)}) K_1 - K_2,$$

w.p. at least $(1 - c/n^2)$, where

$$K_1 = C \sqrt{\log nt} \mathcal{V}^{1/2} + Ct^2(p + \log \bar{n}) \mathcal{V} T_v^{1/2}, \\ K_2 = Ct^2 p^2 \log n \mathcal{V},$$

for some constant C, c . Now we chose $\beta \in (0, 1)$ and let $m := \min_{k \neq l} \frac{2n_k n_l}{n_k + n_l}$. If we suppose

$$\Delta \geq Ctp \sqrt{\log n} \mathcal{V}^{1/2} / (1 - \beta), \quad t \leq C' \sqrt{\log n} / [(p + \log \bar{n}) \mathcal{V}^{1/2} T_v^{1/2}],$$

for some constant C, C' , then we have

$$(1 - \beta) d^2(V^{(l)}, V^{(k)}) - d(V^{(l)}, V^{(k)}) K_1 - K_2 \geq 0, \forall k \neq l,$$

which implies that

$$L \geq \beta d^2(V^{(l)}, V^{(k)}).$$

Define for $k \neq l$,

$$c_j^{(k,l)} := [B_{G_l G_k} 1_{n_k}]_j, \quad j \in G_l, \\ r_i^{(k,l)} := [1_{n_l}^T B_{G_l G_k}]_i, \quad i \in G_k, \\ t^{(k,l)} := 1_{n_l}^T B_{G_l G_k} 1_{n_k}, \\ (B_{G_l G_k}^\#)_{ij} := r_i^{(k,l)} c_j^{(k,l)} / t^{(k,l)}.$$

And define $(B_{G_l G_l}^\#)_{ij} := 0, \forall l$. By setting $\lambda = \frac{\beta}{4} m \Delta^2$, further we have

$$c_j^{(k,l)} \geq \frac{\beta}{2} n_k d^2(V^{(l)}, V^{(k)}), r_i^{(k,l)} \geq \frac{\beta}{2} n_l d^2(V^{(l)}, V^{(k)}), t^{(k,l)} \geq \frac{\beta}{2} n_l n_k d^2(V^{(l)}, V^{(k)}),$$

which implies that $(B_{G_l G_k}^\#)_{ij} > 0, \forall i \in G_k, j \in G_l$. And $[B_{G_l G_k} 1_{n_k}]_j = [B_{G_l G_k}^\# 1_{n_k}]_j$, which means we can construct $B^\#$ based on $[B_{G_l G_k} 1_{n_k}]_j$ with $[B_{G_l G_k} 1_{n_k}]_j = [B_{G_l G_k}^\# 1_{n_k}]_j$. So essentially, they are the same in the sense that we only care about they quantity through $[B_{G_l G_k} 1_{n_k}]_j$. And thus for notation simplicity, we will use the symbol B instead of $B^\#$.

Step 2 (Verify the condition for W_n in (C_2)). Next we would like to find sufficient condition for (C_2) , i.e.,

$$v^T W_n v \geq 0, \forall v \in \Gamma_K := \text{span}\{1_{G_k} : k \in [K]\}^\perp, \|v\| = 1.$$

Note that $v^T W_n v = \lambda - v^T A v - v^T B v \geq \lambda - v^T B v$. And by definition as well as simple calculation we have

$$\begin{aligned} v^T B v &= \sum_{k=1}^K \sum_{l \neq k} \frac{1}{t^{(k,l)}} \left(\sum_{i \in G_k} v_i r_i^{(k,l)} \right) \left(\sum_{j \in G_l} v_j c_j^{(k,l)} \right), \\ \sum_{j \in G_l} v_j c_j^{(k,l)} &= n_k \sum_{j \in G_l} \left(\frac{1}{n_k} \sum_{r \in G_k} d^2(V_j, V_r) - \frac{1}{n_l} \sum_{r \in G_l} d^2(V_j, V_r) \right) v_j. \end{aligned}$$

Further note that

$$\frac{1}{n_k} \sum_{r \in G_k} d^2(V_j, V_r) - \frac{1}{n_l} \sum_{r \in G_l} d^2(V_j, V_r) = d^2(V^{(l)}, V^{(k)}) + E_j^{(k,l)},$$

where

$$\begin{aligned} E_j^{(k,l)} &= \left[\frac{1}{n_k} \sum_{r \in G_k} d^2(V_j, V_r) - d^2(V_j, V^{(k)}) \right] + \left[d^2(V_j, V^{(k)}) - d^2(V^{(l)}, V^{(k)}) \right] \\ &\quad - \frac{1}{n_l} \sum_{r \in G_l} d^2(V_j, V_r). \end{aligned}$$

Then by triangle inequality and throwing away the last term of $E_j^{(k,l)}$, we have

$$\sum_{j \in G_l} v_j c_j^{(k,l)} = n_k \sum_{j \in G_l} E_j^{(k,l)} v_j \leq n_k \sum_{j \in G_l} (E_{1,j}^{(k,l)} + E_{2,j}^{(k,l)}) |v_j|,$$

where

$$\begin{aligned} E_{1,j}^{(k,l)} &= \frac{1}{n_k} \sum_{r \in G_k} d^2(V^{(k)}, V_r) + \left[\frac{2}{n_k} \sum_{r \in G_k} d(V^{(k)}, V_r) d(V_j, V^{(k)}) \right], \\ E_{2,j}^{(k,l)} &= d^2(V^{(l)}, V_j) + 2d(V^{(l)}, V_j) d(V^{(l)}, V^{(k)}). \end{aligned}$$

If we set $\tilde{E}_{h,j}^{(k,l)} = E_{h,j}^{(k,l)} / d(V^{(l)}, V^{(k)})$, $h = 1, 2$, then the inequality can be written as

$$\sum_{j \in G_l} v_j c_j^{(k,l)} \leq n_k d(V^{(l)}, V^{(k)}) \sum_{j \in G_l} (\tilde{E}_{1,j}^{(k,l)} + \tilde{E}_{2,j}^{(k,l)}) |v_j|.$$

By Lemma 15 we know

$$\sum_{j \in G_l} \tilde{E}_{1,j}^{(k,l)} |v_j| \leq C \mathcal{V}^{1/2} p t \sqrt{n_l} \left(\sum_{j \in G_l} v_j^2 \right)^{1/2},$$

w.p. $\geq 1 - cn^{-2}$. And by Lemma 16 we have

$$\sum_{j \in G_l} \tilde{E}_{2,j}^{(k,l)} |v_j| \leq C t \mathcal{V}^{1/2} p (\sqrt{n_l} + \log^2(n)) \left(\sum_{j \in G_l} v_j^2 \right)^{1/2},$$

w.p. $\geq 1 - cn^{-1}$, for some constants C, c . Now if we assume $\min_k n_k \geq C \log^2 n$ and notice that $t^{(k,l)} \geq \frac{\beta}{2} n_l n_k d^2(V^{(l)}, V^{(k)})$, then further we can get

$$\begin{aligned} v^T B v &\leq \sum_{k,l} \frac{n_k n_l}{t^{(k,l)}} \sqrt{n_l} \sqrt{n_k} \left(\sum_{j \in G_l} v_j^2 \right)^{1/2} \left(\sum_{i \in G_k} v_i^2 \right)^{1/2} C t^2 \mathcal{V} p^2 \\ &\leq \frac{C t^2}{\beta} \left(\sum_l \sum_{j \in G_l} v_j^2 \right)^{1/2} \left(\sum_l n_l \right)^{1/2} \left(\sum_k \sum_{i \in G_k} v_i^2 \right)^{1/2} \left(\sum_k n_k \right)^{1/2} \mathcal{V} p^2 \\ &= \frac{C t^2}{\beta} p^2 n \mathcal{V}, \end{aligned}$$

where the second inequality comes from Cauchy-Schwarz inequality. So by assuming

$$\Delta^2 \geq \frac{Ct^2}{\beta^2} \mathcal{V} \cdot p^2 n/m,$$

for some constant C , we have

$$v^T W_n v \geq \lambda - v^T B v \geq \frac{\beta}{4} m \Delta^2 - \frac{Ct^2}{\beta} p^2 n \mathcal{V} > 0.$$

Or it is sufficient to assume

$$\Delta^2 \geq \frac{Ct^2}{\beta^2} \mathcal{V} \cdot p^2 \log n,$$

if $n/m = O(\log n)$. To sum up, if we assume

$$\Delta^2 \geq \frac{Ct^2}{\min\{1-\beta, \beta\}^2} \mathcal{V} \cdot p^2 \log n,$$

then w.p. $\geq 1 - c/n$, we have $(C_1) - (C_4)$ hold by the construction of (λ, B) for some constants C, c . Finally by Lemma 10 we know the solution of SDP Z^* exists uniquely, which is

$$Z^* = \sum_{k \in [K]} \frac{1}{n_k} 1_{G_k} 1_{G_k}^T$$

as desired. ■

Remarks. In our theorem, we focus on the relation between minimum cluster distance $\bar{\Delta}$ with number of distributions n , which should be tight enough in the sense that $\bar{\Delta} \asymp \sqrt{\log n}$. This is the same order for the cut-off of exact recovery of SDP for Euclidean case from Chen and Yang [2021].

On the other hand, one sufficient condition for $V_i, i = 1, \dots, n$ to be psd is $1 - t \max_i \|X_i\|_{op} > 0$, which will hold w.p. $\geq 1 - c/n^2$ if $t \leq C/[\sqrt{p} + \sqrt{\log n}]$ for some constant C, c . Recall from our assumption,

$$t \leq c\sqrt{\log n}/[(p + \log \bar{n})\mathcal{V}^{1/2}T_v^{1/2}] \leq c\sqrt{\log n}/(p + \log \bar{n}),$$

for some constant, since $T_v = \max_k \text{Tr}((V^{(k)})^{-1}) \geq p/\min_k \|V^{(k)}\|_{op}$. This indicates that our bound for t guarantees V_i to be psd w.p. $\geq 1 - c/n^2$ as $n \asymp \bar{n}$. One may apply triangle inequality directly to Lemma 14 to get the upper bound of t with less order in p , which is of less concern in our theorem, where we put more emphasis on the order in n .

D.3.2 Proofs of lemmas.

Before proving Lemma 14, let us first look at the Taylor expansion for psd matrix.

Lemma 11 (Taylor expansion for psd matrix) (Theorem 1.1 in Del Moral and Niclas [2017]). The square root function $\varphi : Q \in \mathcal{S}_r^+ \mapsto Q^{1/2}$ is Fréchet differentiable at any order on \mathcal{S}_r^+ with the first order derivative given for any $(A, H) \in \mathcal{S}_r^+ \times \mathcal{S}_r$ by the formula

$$\nabla \varphi(A) \cdot H = \int_0^\infty e^{-t\varphi(A)} H e^{-t\varphi(A)} dt,$$

where $\mathcal{S}_r^+, \mathcal{S}_r$ are the positive semi-definite matrix and symmetric matrix respectively. The higher order derivatives are defined inductively for any $n \geq 2$ by

$$\nabla^n \varphi(A) \cdot H = -\nabla \varphi(A) \cdot \left[\sum_{p+q=n-2 \& p, q \geq 0} \frac{n!}{(p+1)!(q+1)!} [\nabla^{p+1} \varphi(A) \cdot H][\nabla^{q+1} \varphi(A) \cdot H] \right].$$

Again from the same paper, we have the Taylor expansion for $\varphi(A)$:

$$\varphi(A + H) = \varphi(A) + \sum_{1 \leq k \leq n} \frac{1}{k!} \nabla^k \varphi(A) \cdot H + \bar{\nabla}^{n+1} \varphi[A, H],$$

with

$$\bar{\nabla}^{n+1} \varphi[A, H] := \frac{1}{n!} \int_0^1 (1 - \epsilon)^n \nabla^{n+1} \varphi(A + \epsilon H) \cdot H d\epsilon.$$

Corollary 12 (Decomposition of Wasserstein distance for Gaussians). If we choose $n = 1$ in Lemma 11, we have for $k \neq l, j \in G_l^*$, and under the assumptions in the Theorem, the following expansion holds.

$$\begin{aligned}
& d^2(V_j, V^{(k)}) - d^2(V_j, V^{(l)}) \\
&= d^2(V^{(l)}, V^{(k)}) + \left\langle \mathcal{A}(V^{(l)}, V^{(k)}), t(X_j V^{(l)} + V^{(l)} X_j) + t^2 X_j V^{(l)} X_j \right\rangle \\
& - d^2(V_j, V^{(l)}) - \Delta_0, \\
& \frac{1}{n_k} \sum_{r \in G_k} d^2(V_j, V_r) - d^2(V_j, V^{(k)}) \\
&= \left\langle \mathcal{A}(V_j, V^{(k)}), \frac{1}{n_k} \sum_{r \in G_k} t(X_r V^{(k)} + V^{(k)} X_r) + t^2 X_r V^{(k)} X_r \right\rangle - \Delta_1,
\end{aligned}$$

where $\mathcal{A}(U, V) := Id - U^{1/2}(U^{1/2} V U^{1/2})^{-1/2} U^{1/2}$, for U, V : psd. And $\Delta_0 \leq 0, \Delta_1 \leq 0$, which are extra terms (high order terms in Lemma 11).

Proof. By definition we know $d^2(V, U) = W_2^2(\nu, \mu)$, where $\nu \sim N(0, V), \mu \sim N(0, U)$. Thus

$$d^2(V, U) = \text{Tr}(V) + \text{Tr}(U) - 2\text{Tr}[\sqrt{V^{1/2} U V^{1/2}}].$$

So we have

$$\begin{aligned}
& d^2(V_j, V^{(k)}) - d^2(V^{(k)}, V^{(l)}) \\
&= \text{Tr}[V_j - V^{(l)}] - 2\text{Tr} \left[\sqrt{(V^{(k)})^{1/2} V_j (V^{(k)})^{1/2}} - \sqrt{(V^{(k)})^{1/2} V^{(l)} (V^{(k)})^{1/2}} \right].
\end{aligned}$$

On the other hand, by definition we know $V_j = (I + tX_j)V^{(l)}(I + tX_j) = V^{(l)} + t(X_j V^{(l)} + V^{(l)} X_j) + t^2 X_j V^{(l)} X_j$. Then by Lemma 11 and note the second order remainder term is always negative semi-definite, we can directly get the results by first order Taylor expansion. ■

Lemma 13 (Norm for operator \mathcal{A}). We conclude that for any U, V : psd, we have

$$\|\mathcal{A}(U, V) \cdot V^{1/2}\|_F^2 = \|V^{1/2} \cdot \mathcal{A}(U, V)\|_F^2 = d^2(U, V).$$

Proof. Suppose we have the SVD

$$U^{1/2} V^{1/2} = Q_1^T \Sigma Q_2,$$

then we have

$$\begin{aligned}
\mathcal{A}(U, V) \cdot V^{1/2} &= (I - U^{1/2}(U^{1/2} V U^{1/2})^{-1/2}) V^{1/2} \\
&= V^{1/2} - U^{1/2} Q_1^T Q_2,
\end{aligned}$$

which implies that

$$\begin{aligned}
\|\mathcal{A}(U, V) \cdot V^{1/2}\|_F^2 &= \text{Tr}(V) + \text{Tr}(U) - 2\text{Tr}(V^{1/2} U^{1/2} Q_1^T Q_2) \\
&= \text{Tr}(V) + \text{Tr}(U) - 2\text{Tr}(Q_2^T \Sigma Q_2) \\
&= \text{Tr}(V) + \text{Tr}(U) - 2\text{Tr}(\sqrt{U^{1/2} V U^{1/2}}).
\end{aligned}$$

Lemma 14 (Lower bound for L). Recall that L equals

$$\frac{1}{2} \left[\frac{1}{n_l^2} \sum_{s, r \in G_l} d^2(V_s, V_r) - \frac{1}{n_k^2} \sum_{s, r \in G_k} d^2(V_s, V_r) \right] + \left[\frac{1}{n_k} \sum_{r \in G_k} d^2(V_j, V_r) - \frac{1}{n_l} \sum_{r \in G_l} d^2(V_j, V_r) \right],$$

we have

$$L \geq d^2(V^{(l)}, V^{(k)}) - d(V^{(l)}, V^{(k)})K_1 - K_2,$$

w.p. at least $(1 - c/n^2)$, where

$$\begin{aligned} K_1 &= C\sqrt{\log nt}\mathcal{V}^{1/2} + Ct^2(p + \log \bar{n})\mathcal{V}T v^{1/2}, \\ K_2 &= Ct^2 p^2 \log n\mathcal{V}, \end{aligned}$$

for some constant C, c .

Proof. First note that we can decompose the term into three terms:

$$\frac{1}{n_k} \sum_{r \in G_k} d^2(V_j, V_r) - \frac{1}{n_l} \sum_{r \in G_l} d^2(V_j, V_r) = U_1 - U_2 + U_3,$$

where

$$U_1 := \frac{1}{n_k} \sum_{r \in G_k} d^2(V_j, V_r) - d^2(V_j, V^{(k)}),$$

$$U_2 := \frac{1}{n_l} \sum_{r \in G_l} d^2(V_j, V_r) - d^2(V_j, V^{(l)})$$

$$U_3 := d^2(V_j, V^{(k)}) - d^2(V_j, V^{(l)}).$$

If we further define $U_0 := \frac{1}{2} \left[\frac{1}{n_l^2} \sum_{s,r \in G_l} d^2(V_s, V_r) - \frac{1}{n_k^2} \sum_{s,r \in G_k} d^2(V_s, V_r) \right]$, then we have

$$L = U_0 + U_1 - U_2 + U_3.$$

From Corollary 12 we know U_1 and U_2 can be lower bounded by throwing out the remainders Δ_1, Δ_2 , i.e.,

$$\begin{aligned} U_1 &= \frac{1}{n_k} \sum_{r \in G_k} d^2(V_j, V_r) - d^2(V_j, V^{(k)}) \\ &\geq \left\langle \mathcal{A}(V_j, V^{(k)}), \frac{1}{n_k} \sum_{r \in G_k} t(X_r V^{(k)} + V^{(k)} X_r) + t^2 X_r V^{(k)} X_r \right\rangle, \end{aligned}$$

$$\begin{aligned} U_3 &= d^2(V_j, V^{(k)}) - d^2(V_j, V^{(l)}) \\ &\geq d^2(V^{(l)}, V^{(k)}) + \left\langle \mathcal{A}(V^{(l)}, V^{(k)}), t(X_j V^{(l)} + V^{(l)} X_j) + t^2 X_j V^{(l)} X_j \right\rangle \\ &\quad - d^2(V_j, V^{(l)}). \end{aligned}$$

As for the U_0 and U_3 , we choose to use triangle inequality to get a rough bound, i.e., by noting $d(V_j, V_r) \leq d(V_j, V^{(l)}) + d(V_r, V^{(l)})$, we have

$$\begin{aligned} U_2 &= \frac{1}{n_l} \sum_{r \in G_l} d^2(V_j, V_r) - d^2(V_j, V^{(l)}) \\ &\leq \frac{1}{n_l} \sum_{r \in G_l} d^2(V^{(l)}, V_r) + \frac{2}{n_l} d(V^{(l)}, V_r) \sum_{r \in G_l} d(V_j, V^{(l)}). \end{aligned}$$

And

$$\begin{aligned} U_0 &= \frac{1}{2} \left[\frac{1}{n_l^2} \sum_{s,r \in G_l} d^2(V_s, V_r) - \frac{1}{n_k^2} \sum_{s,r \in G_k} d^2(V_s, V_r) \right] \\ &\geq -\frac{1}{2} \frac{1}{n_l^2} \sum_{s,r \in G_k} (d(V_s, V^{(k)}) + d(V_r, V^{(k)}))^2 \\ &\geq -\frac{2}{n_l} \sum_{r \in G_k} d^2(V^{(k)}, V_r). \end{aligned}$$

For the RHS of the inequality for U_1 , it can be divided into two parts.

$$Z_1^1 := \left\langle \mathcal{A}(V_j, V^{(k)}), \frac{1}{n_k} \sum_{r \in G_k} t(X_r V^{(k)} + V^{(k)} X_r) \right\rangle$$

and

$$Z_2^1 := \left\langle \mathcal{A}(V_j, V^{(k)}), t^2 \frac{1}{n_k} \sum_{r \in G_k} X_r V^{(k)} X_r \right\rangle.$$

the first part is a Gaussian distribution whose variance can be bounded by $c_1 t^2 \|\mathcal{A}(V_j, V^{(k)}) V^{(k)}\|_F^2 / n_k$, for some constant c_1 . By Gaussian tail bound $P(|N(0, 1)| > u) \leq e^{-u^2/2}, \forall u > 0$ and Lemma 13, we have

$$\begin{aligned} |Z_1^1| &\leq c_2 t \sqrt{\log n} \|V^{(k)}\|^{1/2} / \sqrt{n_k} \cdot d(V_j, V^{(k)}) \\ &\leq c_2 t \sqrt{\log n} \mathcal{V}^{1/2} \cdot d(V_j, V^{(k)}), \end{aligned}$$

w.p. $\geq 1 - c_3/n^2$, for some constant c_2, c_3 . On the other hand,

$$\begin{aligned} |Z_2^1| &= t^2 \left| \left\langle \mathcal{A}(V_j, V^{(k)}) (V^{(k)})^{1/2}, \frac{1}{n_k} \sum_{r \in G_k} X_r V^{(k)} X_r (V^{(k)})^{-1/2} \right\rangle \right| \\ &\leq t^2 \left\| \frac{1}{n_k} \sum_{r \in G_k} X_r V^{(k)} X_r (V^{(k)})^{-1/2} \right\|_F \cdot d(V_j, V^{(k)}) \\ &\leq t^2 \frac{1}{n_k} \sum_{r \in G_k} \|X_r\|^2 \|V^{(k)}\| \left\| (V^{(k)})^{-1/2} \right\|_F \cdot d(V_j, V^{(k)}) \\ &\leq t^2 \max_{r \in G_k} \|X_r\|^2 \mathcal{V} T v^{1/2} \cdot d(V_j, V^{(k)}) \\ &\leq c_4 t^2 (p + \log n) \mathcal{V} T v^{1/2} \cdot d(V_j, V^{(k)}), \end{aligned}$$

w.p. $\geq 1 - c_5/n^2$, for some constant c_4, c_5 . The last inequality can be implied from union bound and Corollary 4.4.8 in Vershynin [2018]:

$$\|X_r\| \leq C(\sqrt{p} + u), \quad \text{w.p.} \geq 1 - 4e^{-u^2}.$$

Now by combining Z_1^1, Z_2^1 we have

$$\begin{aligned} U_1 &\geq Z_1^1 + Z_2^1 \\ &\geq - \left[c_2 t \sqrt{\log n} \mathcal{V}^{1/2} + c_4 t^2 (p + \log n) \mathcal{V} T v^{1/2} \right] \cdot d(V_j, V^{(k)}), \end{aligned}$$

w.p. $\geq 1 - (c_3 + c_5)/n^2$.

For U_0 , we have

$$\begin{aligned} U_0 &\geq -\frac{2}{n_k} \sum_{r \in G_k} d^2(V^{(k)}, V_r) \\ &= -\frac{2t^2}{n_k} \sum_{r \in G_k} \text{Tr}(X_r V^{(k)} X_r) \\ &\geq -2t^2 \mathcal{V} \frac{1}{n_k} \sum_{r \in G_k} \text{Tr}(X_r^2) \\ &\geq -c_6 t^2 \mathcal{V} p^2, \end{aligned}$$

w.p. $\geq 1 - c_7/n^2$ for some constant c_6, c_7 . The equation is a direct result by definition of Wasserstein distance for Gaussians:

$$d^2(V^{(k)}, V_r) = \text{Tr}(V^{(k)}) + \text{Tr}(V_r) - 2\text{Tr}(\sqrt{(V^{(k)})^{1/2} V_r (V^{(k)})^{1/2}}).$$

Note here

$$\begin{aligned}\sqrt{(V^{(k)})^{1/2}V_r(V^{(k)})^{1/2}} &= \sqrt{(V^{(k)})^{1/2}(I + tX_r)V^{(k)}(I + tX_r)(V^{(k)})^{1/2}} \\ &= (V^{(k)})^{1/2}(I + tX_r)(V^{(k)})^{1/2}.\end{aligned}$$

The last inequality can be derived through Bernstein's inequality (Theorem 2.8.2 in Vershynin [2018]) by noting that $\text{Tr}(X_r^2)$ is sub-exponential with mean $\mathbb{E}(\text{Tr}(X_r^2)) = p^2$. Similar to the argument for U_0, U_1 , after we apply high-dimensional bound for sub-Gaussian or sub-exponential distributions we can get bound for U_2, U_3 :

$$\begin{aligned}U_2 &\leq \frac{1}{n_l} \sum_{r \in G_l} d^2(V^{(l)}, V_r) + \frac{2}{n_l} \sum_{r \in G_l} d(V_r, V^{(l)})d(V^{(l)}, V_j) \\ &\leq c_8 t^2 \mathcal{V} p^2 \log n,\end{aligned}$$

w.p. $\geq 1 - c_9/n^2$, for some constant c_8, c_9 .

$$\begin{aligned}U_3 &\geq d^2(V^{(l)}, V^{(k)}) + \left\langle \mathcal{A}(V^{(l)}, V^{(k)}), t(X_j V^{(l)} + V^{(l)} X_j) + t^2 X_j V^{(l)} X_j \right\rangle \\ &\quad - d^2(V_j, V^{(l)}) \\ &\geq d^2(V^{(l)}, V^{(k)}) - \left[c_2 t \sqrt{\log n} \mathcal{V}^{1/2} + c_4 t^2 (p + \log \bar{n}) \mathcal{V} T v^{1/2} \right] \cdot d(V^{(l)}, V^{(k)}) \\ &\quad - c_{10} t^2 (p + \log n) p \mathcal{V},\end{aligned}$$

w.p. $\geq 1 - c_{11}/n^2$, for some constant c_{10}, c_{11} . Lastly, by noting $d(V_j, V^{(k)}) \leq d(V^{(l)}, V^{(k)}) + d(V_j, V^{(l)})$ in U_1 , and combine them together we have

$$\begin{aligned}L &= U_0 + U_1 - U_2 + U_3 \\ &\geq d^2(V^{(l)}, V^{(k)}) - d(V^{(l)}, V^{(k)}) K_1 - K_2,\end{aligned}$$

w.p. at least $(1 - c/n^2)$, where

$$\begin{aligned}K_1 &= C \sqrt{\log n} \mathcal{V}^{1/2} + C t^2 (p + \log \bar{n}) \mathcal{V} T v^{1/2}, \\ K_2 &= C t^2 p^2 \log n \mathcal{V},\end{aligned}$$

for some constant C, c . ■

Lemma 15 ($\tilde{E}_{1,j}^{(k,l)}$ upper bound). Suppose $v \in \Gamma_K := \text{span}\{1_{G_k} : k \in [K]\}^\perp$, $\|v\| = 1$. Let

$$E_{1,j}^{(k,l)} = \frac{1}{n_k} \sum_{r \in G_k} d^2(V^{(k)}, V_r) + \left[\frac{2}{n_k} \sum_{r \in G_k} d(V^{(k)}, V_r) d(V_j, V^{(k)}) \right],$$

and $\tilde{E}_{1,j}^{(k,l)} = E_{1,j}^{(k,l)} / d(V^{(l)}, V^{(k)})$. Then w.p. $\geq 1 - n^{-2}$, we have

$$\sum_{j \in G_l} \tilde{E}_{1,j}^{(k,l)} |v_j| \leq C \mathcal{V}^{1/2} p t \sqrt{n_l} \left(\sum_{j \in G_l} v_j^2 \right)^{1/2},$$

Proof. Note $E(\text{Tr}(X_r^2)) = p^2$, $E(\sqrt{\text{Tr}(X_r^2)}) \leq \sqrt{E(\text{Tr}(X_r^2))} = p$ by Jensen's inequality. From high-dimension bound for sub-exponential and sub-Gaussian (Hoeffding's inequality and Bernstein's inequality) we have that w.p. $\geq 1 - c/n^2$,

$$\begin{aligned}\frac{1}{n_k} \sum_{r \in G_k} d^2(V^{(k)}, V_r) &= \frac{1}{n_k} \sum_{r \in G_k} \text{Tr}(X_r^2 V^{(k)}) \leq C \mathcal{V} p^2 t^2, \\ \frac{1}{n_k} \sum_{r \in G_k} d(V^{(k)}, V_r) &= \frac{1}{n_k} \sum_{r \in G_k} \sqrt{\text{Tr}(X_r^2 V^{(k)})} \leq C \mathcal{V}^{1/2} p t,\end{aligned}$$

for some constants C, c . Suppose that $d(V^{(l)}, V^{(k)}) \geq C_0 t \mathcal{V}^{1/2} \sqrt{\log n} p$, for some fixed constant C_0 . Then we have w.p. $\geq 1 - c/n^2$

$$d(V_j, V^{(k)}) \leq d(V_j, V^{(l)}) + d(V^{(l)}, V^{(k)}) \leq C t p \sqrt{\log n} \mathcal{V}^{1/2} + d(V^{(l)}, V^{(k)}) \leq C d(V^{(l)}, V^{(k)}),$$

for some large constant C . So we have w.p. $\geq 1 - c/n^2$

$$\sum_{j \in G_l} \tilde{E}_{1,j}^{(k,l)} |v_j| \leq C\mathcal{V}^{1/2} p t \sum_{j \in G_l} |v_j| \leq C\mathcal{V}^{1/2} p t \sqrt{n_l} \left(\sum_{j \in G_l} v_j^2 \right)^{1/2},$$

where $\mathcal{V} = \max_k \|V^{(k)}\|$, for some large constant C . ■

Lemma 16 ($\tilde{E}_{2,j}^{(k,l)}$ **upper bound**). Suppose $v \in \Gamma_K := \text{span}\{1_{G_k} : k \in [K]\}^\perp$, $\|v\| = 1$. Let

$$E_{2,j}^{(k,l)} = d^2(V^{(l)}, V_j) + 2d(V^{(l)}, V_j)d(V^{(l)}, V^{(k)}).$$

and $\tilde{E}_{2,j}^{(k,l)} = E_{2,j}^{(k,l)} / d(V^{(l)}, V^{(k)})$. Then w.p. $\geq 1 - n^{-1}$, we have

$$\sum_{j \in G_l} \tilde{E}_{2,j}^{(k,l)} |v_j| \leq Ct\mathcal{V}^{1/2} p (\sqrt{n_l} + \log^2(n)) \left(\sum_{j \in G_l} v_j^2 \right)^{1/2},$$

Proof. First we make the following claim:

Claim 17. Following the above setting, w.p. $\geq 1 - cn^{-1}$, we have

$$\sum_{j \in G_l} d^2(V^{(l)}, V_j) |v_j| \leq Ct^2 \mathcal{V} p^2 (\sqrt{n_l} + \log(n)^2) \left(\sum_{j \in G_l} v_j^2 \right)^{1/2}, \quad (24)$$

$$\sum_{j \in G_l} d(V^{(l)}, V_j) |v_j| \leq Ct\mathcal{V}^{1/2} p \sqrt{n_l} \left(\sum_{j \in G_l} v_j^2 \right)^{1/2}, \quad (25)$$

for some large constant C .

If the claim holds, by plugging in the lower bound for Δ in the assumption, we have

$$\begin{aligned} \sum_{j \in G_l} \tilde{E}_{2,j}^{(k,l)} |v_j| &\leq \frac{Ct^2 \mathcal{V} p^2 (\sqrt{n_l} + \log(n)^2)}{C_0 t \mathcal{V}^{1/2} p \sqrt{\log n}} \left(\sum_{j \in G_l} v_j^2 \right)^{1/2} + Ct\mathcal{V}^{1/2} p \sqrt{n_l} \left(\sum_{j \in G_l} v_j^2 \right)^{1/2} \\ &\leq Ct\mathcal{V}^{1/2} p (\sqrt{n_l} + \log^2(n)) \left(\sum_{j \in G_l} v_j^2 \right)^{1/2} \end{aligned}$$

Proof of the claim. First we look at (25):

$$\sum_{j \in G_l} d(V^{(l)}, V_j) |v_j| \leq t\mathcal{V}^{1/2} \sum_{j \in G_l} \sqrt{\text{Tr}(X_j^2)} |v_j|.$$

By Theorem 2.6.3 (General Hoeffding's inequality) in Vershynin [2018] we have w.p. $\geq 1 - c/n^2$,

$$\sum_{j \in G_l} \sqrt{\text{Tr}(X_j^2)} |v_j| \leq p \sum_{j \in G_l} |v_j| + Cp\sqrt{n_l} \left(\sum_{j \in G_l} v_j^2 \right)^{1/2},$$

for some constant C . i.e., w.p. $\geq 1 - c/n^2$,

$$\sum_{j \in G_l} d(V^{(l)}, V_j) |v_j| \leq Ct\mathcal{V}^{1/2} p \sqrt{n_l} \left(\sum_{j \in G_l} v_j^2 \right)^{1/2},$$

for some constant C . Next we will show (24). First note that $d^2(V^{(l)}, V_j) \leq t^2 \mathcal{V} \text{Tr}(X_j^2)$, let

$$G_1(v) = \left| \sum_{j \in G_l} [\text{Tr}(X_j^2) - \mathbb{E} \text{Tr}(X_j^2)] |v_j| \right|,$$

then

$$\sum_{j \in G_l} d^2(V^{(l)}, V_j) |v_j| \leq t^2 \mathcal{V} G_1(v) + t^2 \mathcal{V} p^2 \sqrt{n_l} \left(\sum_{j \in G_l} v_j^2 \right)^{1/2}.$$

W.O.L.G., we may assume $v \in \mathbb{V} := \{v \in \Gamma_K : \|v\| = 1\}$, $\|G_1\|_{\mathbb{V}} := \sup_{v \in \mathbb{V}} |G_1(v)|$. Then by Theorem 4 in Adamczak [2008] we know

$$\mathbb{P}(\|G_1\|_{\mathbb{V}} \geq 2\mathbb{E}\|G_1\|_{\mathbb{V}} + s) \leq \exp\left(-\frac{s^2}{3\tau_1^2}\right) + 3 \exp\left(-\frac{s}{3\|M_1\|_{\psi_1}}\right),$$

where

$$\tau_1^2 = \sup_{v \in \mathbb{V}} \sum_{j \in G_l} v_j^2 \mathbb{E}[\text{Tr}(X_j^2) - \mathbb{E} \text{Tr}(X_j^2)]^2 \leq \mathbb{E}[\text{Tr}(X_j^2)]^2 \leq p^4,$$

$$M_1 = \max_{j \in G_l, v \in \mathbb{V}} |v_j [\text{Tr}(X_j^2) - \mathbb{E} \text{Tr}(X_j^2)]| \leq \max_{j \in G_l} |[\text{Tr}(X_j^2) - \mathbb{E} \text{Tr}(X_j^2)]|.$$

By maximal inequality (Lemma 2.2.2 in van der Vaart and Wellner [1996]) we have

$$\|M_1\|_{\psi_1} \leq C \log(n_l) \max_{j \in G_l} \|[\text{Tr}(X_j^2) - \mathbb{E} \text{Tr}(X_j^2)]\|_{\psi_1} \leq C \log(n_l) p^2.$$

So by choosing $s = C \log^2(n) p^2$, we have w.p. $\geq 1 - c/n$,

$$G_1(v) \leq 2\mathbb{E}\|G_1\|_{\mathbb{V}} + C \log^2(n) p^2,$$

for some C, c . On the hand,

$$\begin{aligned} \mathbb{E}\|G_1\|_{\mathbb{V}} &= \mathbb{E} \left| \sum_{j \in G_l} [\text{Tr}(X_j^2) - \mathbb{E} \text{Tr}(X_j^2)] |v_j| \right| \\ &\leq \sum_{j \in G_l} \mathbb{E} |[\text{Tr}(X_j^2) - \mathbb{E} \text{Tr}(X_j^2)]| |v_j| \\ &\leq 2\mathbb{E} |\text{Tr}(X_1^2)| \sqrt{n_l} \left(\sum_{j \in G_l} v_j^2 \right)^{1/2} \\ &= 2p^2 \sqrt{n_l} \left(\sum_{j \in G_l} v_j^2 \right)^{1/2}. \end{aligned}$$

So w.p. $\geq 1 - cn^{-1}$, we have

$$\sum_{j \in G_l} d^2(V^{(l)}, V_j) |v_j| \leq Ct^2 \mathcal{V} p^2 (\sqrt{n_l} + \log(n)^2) \left(\sum_{j \in G_l} v_j^2 \right)^{1/2}.$$

■